

Numerical solution of scalar conservation laws with random flux functions

Report**Author(s):**

Mishra, Siddhartha; Risebro, Nils Henrik; Schwab, Christoph; Tokareva, Svetlana

Publication date:

2012-10

Permanent link:

<https://doi.org/10.3929/ethz-a-010386357>

Rights / license:

In Copyright - Non-Commercial Use Permitted

Originally published in:

SAM Research Report 2012-35

Funding acknowledgement:

247277 - Automated Urban Parking and Driving (EC)

Numerical solution of scalar conservation laws with random flux functions

S. Mishra and N. H. Risebro and Ch. Schwab and S. Tokareva

Research Report No. 2012-35

October 2012

Latest revision: September 2014

Seminar für Angewandte Mathematik
Eidgenössische Technische Hochschule
CH-8092 Zürich
Switzerland

NUMERICAL SOLUTION OF SCALAR CONSERVATION LAWS WITH RANDOM FLUX FUNCTIONS

SIDDHARTHA MISHRA, NILS HENRIK RISEBRO, CHRISTOPH SCHWAB,
AND SVETLANA TOKAREVA

ABSTRACT. We consider scalar hyperbolic conservation laws in several space dimensions, with a class of random (and parametric) flux functions. We propose a Karhunen–Loève expansion on the state space of the random flux. For random flux functions which are continuously differentiable with respect to the state variable u , we prove the existence of a unique random entropy solution. Using a Karhunen–Loève spectral decomposition of the random flux into principal components with respect to the state variables, we introduce a family of parametric, deterministic entropy solutions on high-dimensional parameter spaces. We prove bounds on the sensitivity of the parametric and of the random entropy solutions on the Karhunen–Loève parameters. We also outline the convergence analysis for two classes of discretization schemes, the Multi-Level Monte-Carlo Finite-Volume Method (MLMCFVM) developed in [21, 23, 22], and the stochastic collocation Finite Volume Method (SCFVM) of [29].

1. INTRODUCTION

Many problems in physics and engineering are modeled by hyperbolic systems of conservation or balance laws. As examples for these equations, we mention only the Shallow Water Equations of hydrology, the Euler Equations for inviscid, compressible flow and the Magnetohydrodynamic (MHD) equations of plasma physics, see, e.g. [7, 12].

The simplest example for a system of hyperbolic conservation laws is the scalar (single) conservation law:

$$(1.1) \quad \frac{\partial u}{\partial t} + \sum_{j=1}^d \frac{\partial}{\partial x_j} (f_j(u)) = 0, \quad x = (x_1, \dots, x_d) \in \mathbb{R}^d, \quad t > 0.$$

Here the unknown is $u : \mathbb{R}^d \mapsto \mathbb{R}$ and f_j is the flux function in the j -th dimension.

Solutions of (1.1) develop discontinuities in finite time even when the initial data is smooth and must be interpreted in the weak sense. Weak solutions to (1.1) are not unique, so (1.1) is augmented with additional admissibility criteria, or *entropy conditions*, [7, 28]. Well-posedness of entropy solutions in the scalar case in several space dimensions was obtained by Kruzhkov.

Numerical methods for approximating entropy solutions of systems of conservation laws have undergone extensive development and many efficient methods are available, see [9, 12, 13, 19] and the references therein. In particular, finite volume methods are frequently employed to approximate systems of conservation laws.

Date: September 12, 2014.

1991 *Mathematics Subject Classification.* 65N30,65M06,35L65.

Acknowledgement. This work is performed as part of ETH interdisciplinary research grant CH1-03 10-1. The work of CS was supported in part by ERC FP7 grant no. AdG 247277. The work of NHR was performed while visiting SAM during a sabbatical in the academic year 2011/12.

This *classical* paradigm for designing efficient numerical schemes assumes that *data i.e., initial data and flux function for the system are known exactly.*

In many situations of practical interest, however, these data are not known exactly due to inherent uncertainty in modelling and measurements of physical parameters such as, for example, the specific heats in the equation of state for compressible gases, resistivity in MHD etc. Often, the initial data and the flux function are known only up to certain statistical quantities of interest like the mean, variance, higher moments, and in some cases, the law of the stochastic initial data. In such cases, a mathematical formulation of (1.1) is required which allows for *random problem data*. The problem of random initial data was considered in [21], and the existence and uniqueness of a random entropy solution was shown, and a convergence analysis for MLMC FV discretizations was given. Efficient MLMC discretization of balance laws with random source terms was investigated in [22].

We mention that the present work as well as [21, 22] considered *correlated random inputs* which typically occur in engineering applications; SCLs with random inputs have been considered before, but generally with *white noise*, i.e., spatially and temporally uncorrelated random inputs in [16, 15, 8, 32, 33].

The first aim of this paper is *to develop an appropriate mathematical framework of random entropy solutions for scalar hyperbolic conservation laws with random flux functions with correlated random perturbations.* As well-posedness results in the deterministic case appear to be available only in the scalar case, we focus our discussion on this particular case for our theoretical development. We define random entropy solutions and prove well-posedness result, significantly extending [21] where the initial data was the only random input and underpinning the extensive numerical results reported in [23, 22].

The second aim of this paper is the *analysis and implementation of efficient deterministic numerical solution methods for scalar conservation laws with uncertain flux functions* in multiple space dimensions. We remark that the efficient numerical solution of *systems* of conservation laws with random source terms by multilevel Monte-Carlo methods has been addressed in [22].

We propose and analyze two methods to this end: first, statistical sampling techniques of Monte Carlo (MC) and of Multilevel Monte Carlo (MLMC) type and, second, a deterministic “stochastic collocation Finite Volume Method” (SCFVM for short).

Both of these methods are “non-intrusive”, very easy to code and to parallelize, and well suited for random solutions with low spatial regularity. This situation is typical in conservation laws where discontinuities are generic. This low regularity poses serious challenges to the design of efficient *so-called stochastic Galerkin methods* which are based on *generalized Polynomial Chaos* (gPC for short) expansions of the random solution. Although these methods have been extensively developed, see [1, 4, 20, 30, 24, 31] and other references therein, they are more intrusive, generally harder to implement and more difficult to parallelize than MC methods. Due to the limited smoothness of parametric solutions (shocks forming in physical space will propagate into the parameter domain), convergence rates achieved with stochastic Galerkin approximations as proposed in [24] and references therein, are limited.

Efficient statistical sampling methods of the Multi-level Monte Carlo (MLMC) type were proposed in [21] for SCLs with random initial data. This family of methods was introduced by Heinrich for numerical quadrature [14] and by Giles

in the context of path simulations for stochastic ordinary differential equations [10, 11]. More recently, MLMC finite element methods for elliptic problems with stochastic coefficients were introduced by Barth, Schwab and Zollinger in [2]. More recent papers [21, 23, 22] propose MLMC algorithms for systems of conservation laws and systems of balance laws, with uncertain initial data and with uncertain source terms. One of the aims of the current paper is to extend and analyse the MLMC algorithm for scalar conservation laws with random flux functions. The existence result of random entropy solutions for SCL with bounded random flux functions shown in the present paper is the basis for the recent convergence analysis of Multilevel Monte-Carlo Front-tracking solvers for SCL with bounded random flux functions in [25].

Another class of non-intrusive algorithms for random conservation laws are of the stochastic collocation finite volume method (SCFVM) type proposed in [3], see also [29]. We will consider discretization of SCLs with bounded random flux functions using SCFVM in this paper. Based on a-priori sensitivity estimates in the present paper, we propose a novel anisotropic mesh selection procedure in the stochastic coordinates that serves to reduce the computational complexity of the stochastic FV method considerably.

The remainder of this paper is organized as follows: in Section 2, we introduce some preliminary notions from probability theory and functional analysis. The concept of random entropy solutions is introduced and the scalar hyperbolic conservation law with random initial data and random flux function is shown to be well-posed in Section 3. The MLMCFVM schemes are designed and analyzed in Section 4 SCFVM schemes are presented in Section 5. Finally, illustrative numerical experiments are discussed in Section 6.

2. RANDOM FIELDS

Our mathematical formulation of scalar conservation laws with random data and fluxes will use the concept of random variables taking values in function spaces. For the sake of completeness, we recapitulate basic concepts from Chapter 1 of [6], and then add several remarks on spatial and on temporal correlation functions which will become useful in the ensuing developments. The presentation follows our earlier work [21].

Let (Ω, \mathcal{F}) be a measurable space, with Ω denoting the set of all elementary events, and \mathcal{F} a σ -algebra of all possible events in our probability model. If (E, \mathcal{G}) denotes a second measurable space, then an *E-valued random variable* (or random variable taking values in E) is any mapping $X : \Omega \rightarrow E$ such that the set $\{\omega \in \Omega : X(\omega) \in A\} = \{X \in A\} \in \mathcal{F}$ for any $A \in \mathcal{G}$, i.e., such that X is a \mathcal{G} -measurable mapping from Ω into E .

Assume now that E is a metric space; with the Borel σ -field $\mathcal{B}(E)$, $(E, \mathcal{B}(E))$ is a measurable space and we shall always assume that E -valued random variables $X : \Omega \rightarrow E$ will be $(\mathcal{F}, \mathcal{B}(E))$ measurable. If E is a separable Banach-space with norm $\|\cdot\|_E$ and (topological) dual E^* , then $\mathcal{B}(E)$ is the smallest σ -field of subsets of E containing all sets

$$(2.1) \quad \{x \in E : \varphi(x) \leq \alpha\}, \quad \varphi \in E^*, \quad \alpha \in \mathbb{R}.$$

Hence if E is a separable Banach space, $X : \Omega \rightarrow E$ is an E -valued random variable iff for every $\varphi \in E^*$, $\omega \mapsto \varphi(X(\omega)) \in \mathbb{R}^1$ is an \mathbb{R}^1 -valued random variable. Moreover, we have

Lemma 2.1. *Let E be a separable Banach-space and let $X : \Omega \rightarrow E$ be an E -valued random variable on (Ω, \mathcal{F}) . Then the mapping $\Omega \ni \omega \mapsto \|X(\omega)\|_E \in \mathbb{R}^1$ is measurable.*

Proof. Since E is separable, there exists a sequence $\{\varphi_n\} \subset E^*$ such that for all $x \in E$ holds

$$(2.2) \quad \|x\|_E = \sup_{n \in \mathbb{N}} |\varphi_n(x)|.$$

Hence we find

$$(2.3) \quad \forall \omega \in \Omega : \|X(\omega)\|_E = \sup_{n \in \mathbb{N}} |\varphi_n(X(\omega))|$$

which implies that $\omega \mapsto \|X(\omega)\|_E$ is an \mathbb{R}^1 -valued random variable. \square

The random variable $X : \Omega \rightarrow E$ is called *Bochner integrable* if, for any probability measure \mathbb{P} on the measurable space (Ω, \mathcal{F}) ,

$$(2.4) \quad \int_{\Omega} \|X(\omega)\|_E d\mathbb{P}(\omega) < \infty.$$

Here, a probability measure \mathbb{P} on (Ω, \mathcal{F}) is any σ -additive set function from Ω into $[0, 1]$ such that $\mathbb{P}(\Omega) = 1$, and the resulting measure space $(\Omega, \mathcal{F}, \mathbb{P})$ is a *probability space*. We shall always assume, unless explicitly stated, that $(\Omega, \mathcal{F}, \mathbb{P})$ is complete.

If $X : (\Omega, \mathcal{F}) \rightarrow (E, \mathcal{E})$ is a random variable, $\mathcal{L}(X)$ denotes the *law of X under \mathbb{P}* , i.e.,

$$(2.5) \quad \mathcal{L}(X)(A) = \mathbb{P}(\{\omega \in \Omega : X(\omega) \in A\}) \quad \forall A \in \mathcal{E}.$$

The image measure $\mu_X = \mathcal{L}(X)$ on (E, \mathcal{E}) is called law or distribution of X .

A random variable taking values in E is called *simple* if it can take only finitely many values, i.e., if it has the explicit form (with χ_A the indicator function of $A \in \mathcal{F}$)

$$(2.6) \quad X = \sum_{i=1}^N x_i \chi_{A_i}, \quad A_i \in \mathcal{F}, \quad x_i \in E, \quad N < \infty.$$

We set, for simple random variables X taking values in E and for any $B \in \mathcal{F}$,

$$(2.7) \quad \int_B X(\omega) d\mathbb{P}(\omega) = \int_B X d\mathbb{P} := \sum_{i=1}^N x_i \mathbb{P}(A_i \cap B).$$

By density, for such $X(\cdot)$, and all $B \in \mathcal{F}$,

$$(2.8) \quad \left\| \int_B X(\omega) d\mathbb{P}(\omega) \right\|_E \leq \int_B \|X(\omega)\|_E d\mathbb{P}(\omega).$$

For any random variable $X : \Omega \rightarrow E$ which is Bochner integrable, there exists a sequence $\{X_m\}_{m \in \mathbb{N}}$ of simple random variables such that, for all $\omega \in \Omega$, $\|X(\omega) -$

$X_m(\omega)\|_E \rightarrow 0$ as $m \rightarrow \infty$. Therefore, (2.7) and (2.8) extend in the usual fashion by continuity to any E -valued random variable. We denote the integral

$$(2.9) \quad \int_{\Omega} X(\omega) d\mathbb{P}(\omega) = \lim_{m \rightarrow \infty} \int_{\Omega} X_m(\omega) d\mathbb{P}(\omega) \in E$$

by $\mathbb{E}[X]$ (“expectation” of X). \square

We shall require for $1 \leq p \leq \infty$ Bochner spaces of p -summable random variables X taking values in the Banach-space E . By $L^1(\Omega, \mathcal{F}, \mathbb{P}; E)$ we denote the set of all (equivalence classes of) integrable, E -valued random variables X . We equip it with the norm

$$(2.10) \quad \|X\|_{L^1(\Omega; E)} = \int_{\Omega} \|X(\omega)\|_E d\mathbb{P}(\omega) = \mathbb{E}(\|X\|_E).$$

More generally, for $1 \leq p < \infty$, we define $L^p(\Omega, \mathcal{F}, \mathbb{P}; E)$ as the set of p -summable random variables taking values E and equip it with norm

$$(2.11) \quad \|X\|_{L^p(\Omega; E)} := (\mathbb{E}(\|X\|_E^p))^{1/p}, \quad 1 \leq p < \infty.$$

For $p = \infty$, we denote by $L^\infty(\Omega, \mathcal{F}, \mathbb{P}; E)$ the set of all E -valued random variables which are essentially bounded. This set is a Banach space equipped with the norm

$$(2.12) \quad \|X\|_{L^\infty(\Omega; E)} := \operatorname{ess\,sup}_{\omega \in \Omega} \|X(\omega)\|_E.$$

If $T < \infty$ and $\Omega = [0, T]$, $\mathcal{F} = \mathcal{B}([0, T])$, we write $L^p([0, T]; E)$. Note that for any separable Banach-space E , and for any $r \geq p \geq 1$,

$$(2.13) \quad L^r(0, T; E), C^0([0, T]; E) \in \mathcal{B}(L^p(0, T; E)).$$

3. HYPERBOLIC CONSERVATION LAWS WITH RANDOM FLUX

We review classical results on SCLs with deterministic data, and develop a theory of random entropy solutions for SCLs with a class of random flux functions, proving in particular the existence and uniqueness of a random entropy solution with finite second moments.

We also propose a novel spectral decomposition of the random entropy solutions which is based on a Karhunen–Loève expansion in state space.

3.1. Deterministic scalar hyperbolic conservation laws. We consider the Cauchy problem for scalar conservation laws (SCL) such as (1.1). Introducing the flux function $f(u)$

$$(3.1) \quad f(u) = (f_1(u), \dots, f_d(u)) \in C^1(\mathbb{R}; \mathbb{R}^d), \quad \operatorname{div} f(u) = \sum_{j=1}^d \frac{\partial}{\partial x_j} f_j(u),$$

we may rewrite (1.1) succinctly as

$$(3.2) \quad \frac{\partial u}{\partial t} + \operatorname{div}(f(u)) = 0 \quad \text{for } (x, t) \in \mathbb{R}^d \times \mathbb{R}_+.$$

We supply the SCL (3.2) with initial condition

$$(3.3) \quad u(x, 0) = u_0(x), \quad x \in \mathbb{R}^d.$$

3.2. Entropy Solution. It is well-known that the deterministic Cauchy problem (3.2), (3.3) admits, for each $u_0 \in L^1(\mathbb{R}^d) \cap BV(\mathbb{R})$, a unique entropy solution (see, e.g., [12, 28, 7]). Moreover, for every $t > 0$, $u(\cdot, t) \in L^1(\mathbb{R}^d)$ and the (nonlinear) data-to-solution operator

$$(3.4) \quad S : u_0 \mapsto u(\cdot, t) = S(t)u_0, \quad t > 0$$

has several properties which will be crucial for our subsequent development. To state the properties of $\{S(t)\}_{t \geq 0}$, we introduce some additional notation: for a Banach-space E with norm $\|\circ\|_E$, and for $0 < T \leq +\infty$, denote by $C([0, T]; E)$ the space of bounded and continuous functions from $[0, T]$ with values in E , and by $L^p(0, T; E)$, $1 \leq p \leq +\infty$, the space of strongly measurable functions from $(0, T)$ to E such that for $1 \leq p < +\infty$

$$(3.5) \quad \|v\|_{L^p(0, T; E)} = \left(\int_0^T \|v(t)\|_E^p dt \right)^{\frac{1}{p}},$$

respectively, if $p = \infty$,

$$(3.6) \quad \|v\|_{L^\infty(0, T; E)} = \operatorname{ess\,sup}_{0 \leq t \leq T} \|v(t)\|_E$$

are finite. The following existence result is classical (we refer to, e.g., [12, 13, 18, 9, 19] for a proof).

Theorem 3.1.

- 1) For every $u_0 \in L^\infty(\mathbb{R}^d)$, (3.1) - (3.3) admits a unique entropy solution $u \in L^\infty(\mathbb{R}^d \times (0, T)) := L^\infty(0, T; L^\infty(\mathbb{R}^d))$.
- 2) For every $t > 0$, the (nonlinear) data-to-solution map $S(t)$ given by

$$u(\cdot, t) = S(t)u_0$$

satisfies

- i) $S(t) : L^1(\mathbb{R}^d) \rightarrow L^1(\mathbb{R}^d)$ is a (contractive) Lipschitz map, i.e.,

$$(3.7) \quad \|S(t)u_0 - S(t)v_0\|_{L^1(\mathbb{R}^d)} \leq \|u_0 - v_0\|_{L^1(\mathbb{R}^d)}.$$

- ii) $S(t)$ maps $(L^1 \cap BV)(\mathbb{R}^d)$ into $(L^1 \cap BV)(\mathbb{R}^d)$ and

$$(3.8) \quad TV(S(t)u_0) \leq TV(u_0) \quad \forall u_0 \in (L^1 \cap BV)(\mathbb{R}^d).$$

- iii) For every $u_0 \in (L^\infty \cap L^1)(\mathbb{R}^d)$,

$$(3.9) \quad \|S(t)u_0\|_{L^\infty(\mathbb{R}^d)} \leq \|u_0\|_{L^\infty(\mathbb{R}^d)};$$

$$(3.10) \quad \|S(t)u_0\|_{L^1(\mathbb{R}^d)} \leq \|u_0\|_{L^1(\mathbb{R}^d)}.$$

- iv) The mapping $S(t)$ is a uniformly continuous mapping from $L^1(\mathbb{R}^d)$ into $C([0, \infty); L^1(\mathbb{R}^d))$, and

$$(3.11) \quad \|S(\cdot)u_0\|_{C([0, T]; L^1(\mathbb{R}^d))} = \max_{0 \leq t \leq T} \|S(t)u_0\|_{L^1(\mathbb{R}^d)} \leq \|u_0\|_{L^1(\mathbb{R}^d)}.$$

In our analysis of SCLs with random flux, we will require in particular results on the continuous dependence of entropy solutions on the flux function. In the statement of the following theorem, the (separable) Banach space $C^1(\mathbb{R}, \mathbb{R}^d)$ denotes the space of continuously differentiable functions from \mathbb{R} to \mathbb{R}^d , equipped with the norm $\|f\|_{C^1} = \sup_{v \in \mathbb{R}} \|f(v)\| + \sup_{v \in \mathbb{R}} \|f'(v)\|$, with $\|\circ\|$ denoting some vector-norm on \mathbb{R}^d . We write $|f|_{C^1}$ when only the supremum of the derivative is meant.

Theorem 3.2. ([17, Thm. 4.3]). *Assume $u_0, v_0 \in BV(\mathbb{R}^d) \cap L^1(\mathbb{R}^d)$, and $f(\cdot), g(\cdot) \in C^1(\mathbb{R}; \mathbb{R}^d)$.*

Then the unique entropy solutions u and v of the SCL with initial data u_0, v_0 and with flux functions f and g satisfy the Kruřkov entropy conditions, and the a-priori continuity estimate

$$(3.12) \quad \begin{aligned} \|u(\cdot, t) - v(\cdot, t)\|_{L^1(\mathbb{R}^d)} \\ \leq \|u_0 - v_0\|_{L^1(\mathbb{R}^d)} + t \min\{TV(u_0), TV(v_0)\} \|f - g\|_{C^1(\mathbb{R}; \mathbb{R}^d)} \end{aligned}$$

for every $0 \leq t \leq T$.

3.3. Random Flux. We are in particular interested in the case that the initial data u_0 and the flux functions f_j in (1.1) are uncertain. Since the case of random u_0 was considered in detail in [21], so that we address now in detail the case of random flux. To avoid technicalities, we first address *spatially homogeneous random flux functions* whose realizations are elements of the space $E = C^1(\mathbb{R}; \mathbb{R}^d)$. This space being separable, we define random flux functions in the usual fashion.

Definition 3.3. *A (spatially homogeneous) random flux for the SCL (3.1) - (3.3) is a random field taking values in the separable Banach space $E = C^1(\mathbb{R}; \mathbb{R}^d)$, i.e., a measurable mapping from (Ω, \mathcal{F}) to the measurable space $(C^1(\mathbb{R}; \mathbb{R}^d); \mathcal{B}(C^1(\mathbb{R}; \mathbb{R}^d)))$. A bounded random flux is a random flux whose $C^1(\mathbb{R}^1; \mathbb{R}^d)$ -norm is bounded \mathbb{P} -a.s., i.e.,*

$$(3.13) \quad \exists 0 < B(f) < \infty : \|f(\omega; \cdot)\|_{C^1(\mathbb{R}^1; \mathbb{R}^d)} \leq B(f) \quad \mathbb{P} - a.s. .$$

We observe that a bounded random flux has finite statistical moments of any order. Of particular interest will be the *second moment of a bounded random flux* (i.e., its ‘‘two-point correlation in state-space’’).

Lemma 3.4. *Let f be a bounded random flux as in Definition 3.3 which belongs to $L^2(\Omega; C^1(\mathbb{R}; \mathbb{R}^d))$. Then its covariance function, i.e., its centered second moment defined by*

$$(3.14) \quad \text{Cov}[f](v, v') := \mathbb{E}[(f(\cdot; v) - \mathbb{E}[f(\cdot; v)]) \otimes (f(\cdot; v') - \mathbb{E}[f(\cdot; v')])]$$

is well-defined for all $v, v' \in \mathbb{R}$ and there holds

$$(3.15) \quad \text{Cov}[f] \in C^1(\mathbb{R} \times \mathbb{R}; \mathbb{R}_{sym}^{d \times d})$$

Proof. As a bounded random flux has by definition finite second moments and is, \mathbb{P} -a.s. a Lipschitz continuous function on \mathbb{R} , its expectation $\mathbb{R} \ni v \mapsto \mathbb{E}[f(\cdot; v)] \in C^1(\mathbb{R}; \mathbb{R}^d)$. We have that

$$\|\mathbb{E}[f(\cdot; v)] - \mathbb{E}[f(\cdot; v')]\|_2 \leq B(f)|v - v'|, \quad v, v' \in \mathbb{R} .$$

In particular, therefore, $f(\omega; v) - \mathbb{E}[f(\cdot; v)] \in L^2(\Omega; C^1(\mathbb{R}; \mathbb{R}^d))$. This implies, denoting $\bar{f}(v) = \mathbb{E}[f(\cdot; v)]$, $F = \mathbb{R}_{sym}^{d \times d}$, (recalling our convention that all vectors are column vectors), that for every $v, v' \in \mathbb{R}$ holds

$$\begin{aligned} \|\text{Cov}[f](v, v')\|_F^2 &= \left\| \int_{\Omega} (f(\omega; v) - \bar{f}(v))(f(\omega; v') - \bar{f}(v'))^\top d\mathbb{P}(\omega) \right\|_F^2 \\ &= \sum_{i,j=1}^d \left(\int_{\Omega} (f_i - \bar{f}_i)(\omega; v)(f_j - \bar{f}_j)(\omega; v') d\mathbb{P}(\omega) \right)^2 \end{aligned}$$

$$\leq \int_{\Omega} \|f(\omega; v) - \bar{f}(v)\|_2^2 d\mathbb{P}(\omega) \int_{\Omega} \|f(\omega; v') - \bar{f}(v')\|_2^2 d\mathbb{P}(\omega).$$

Therefore $\text{Cov}[f](v, v')$ is well-defined on $\mathbb{R} \times \mathbb{R}$. Consider now arbitrary states $u, u' \in \mathbb{R}$ and $v, v' \in \mathbb{R}$. Then we may write

$$\begin{aligned} & \|\text{Cov}[f](u, v) - \text{Cov}[f](u', v')\|_F \\ &= \|\text{Cov}[f](u, v) - \text{Cov}[f](u, v') + \text{Cov}[f](u, v') - \text{Cov}[f](u', v')\|_F \\ &\leq \|\text{Cov}[f](u, v) - \text{Cov}[f](u, v')\|_F + \|\text{Cov}[f](u, v') - \text{Cov}[f](u', v')\|_F. \end{aligned}$$

We estimate the first term in this bound as above

$$\begin{aligned} \|\text{Cov}[f](u, v) - \text{Cov}[f](u, v')\|_F^2 &= \left(\int_{\Omega} (f(\omega; u) - \bar{f}(u))(f(\omega; v) - \bar{f}(v))^\top \right. \\ &\quad \left. - (f(\omega; u) - \bar{f}(u))(f(\omega; v') - \bar{f}(v'))^\top d\mathbb{P}(\omega) \right)^2 \\ &= \left(\int_{\Omega} (f(\omega; u) - \bar{f}(u)) \right. \\ &\quad \left. \times [f(\omega; v) - f(\omega; v') - (\bar{f}(v) - \bar{f}(v'))]^\top d\mathbb{P}(\omega) \right)^2 \\ &\leq 2 \int_{\Omega} \|f(\omega; u) - \bar{f}(u)\|_2^2 d\mathbb{P}(\omega) \\ &\quad \times \left(\int_{\Omega} \|f(\omega; v) - f(\omega; v')\|_2^2 d\mathbb{P}(\omega) + \|\bar{f}(v) - \bar{f}(v')\|_2^2 \right) \\ &\leq 4B(f)^2 \int_{\Omega} \|f(\omega; u) - \bar{f}(u)\|_2^2 d\mathbb{P}(\omega) |v - v'|^2. \end{aligned}$$

Proceeding in the same way with the second term, we obtain

$$\|\text{Cov}[f](u, v) - \text{Cov}[f](u', v)\|_F^2 \leq 4B(f)^2 \int_{\Omega} \|f(\omega; v) - \bar{f}(v)\|_2^2 d\mathbb{P}(\omega) |u - u'|^2.$$

Let now

$$C(u, v) = \max \left\{ \left(\int_{\Omega} \|f(\omega; u) - \bar{f}(u)\|_2^2 d\mathbb{P}(\omega) \right)^{1/2}, \left(\int_{\Omega} \|f(\omega; v) - \bar{f}(v)\|_2^2 d\mathbb{P}(\omega) \right)^{1/2} \right\}.$$

Taking square roots and adding the bounds, we obtain

$$\|\text{Cov}[f](u, v) - \text{Cov}[f](u', v')\|_F \leq 2B(f)C(u, v) (|u - u'| + |v - v'|).$$

which implies (3.15). \square

Remark 3.5. *The previous theorem addressed the covariance function for a spatially homogeneous random flux function $f(\omega; u)$. Spatially inhomogeneous flux functions $f(\omega; x, u)$ can be defined analogously, provided their dependence on the spatial coordinate is Lipschitz: they are measurable mappings from (Ω, \mathcal{F}) into $(E, \mathcal{B}(E))$ where $E = \text{Lip}(\mathbb{R}^{d+1}; \mathbb{R}^d)$. If $f \in L^2(\Omega; E)$, its covariance function*

$$\text{Cov}[f](x, v; x', v') := \mathbb{E}[(f(\cdot; x, v) - \mathbb{E}[f](x, v)) \otimes (f(\cdot; x', v') - \mathbb{E}[f](x', v'))]$$

is well-defined as an element of $C^1(\mathbb{R}^{d+1} \times \mathbb{R}^{d+1}; \mathbb{R}_{sym}^{d \times d})$.

3.4. Parametric, deterministic flux. Often, in applications, rather than a bounded random flux function as in Definition 3.3 one is given a *deterministic, parametric flux* function $f(y; u)$ which depends on a vector $y = (y_j)_{j \geq 1}$ of (finitely or infinitely many) parameters in a set U of admissible parameter values.

Definition 3.6. A parametric, deterministic flux function is a function $f(y; u)$ which, for every parameter instance $y \in U$, belongs to $C^1(\mathbb{R}; \mathbb{R}^d)$ and for which there exists a constant $B(f) < \infty$ such that

$$(3.16) \quad \sup_{y \in U} \|f(y; \cdot)\|_{C^1(\mathbb{R}; \mathbb{R}^d)} \leq B(f).$$

We give several examples of parametric, deterministic flux functions.

Example 3.7. Consider a parametric, deterministic flux function which depends on a parameter vector $y \in \mathbb{R}^J$. Let $y_0 \in \mathbb{R}^J$ denote a *nominal parameter value* and denote, for $r > 0$, $U = B_r(y_0) := \{y \in \mathbb{R}^J \mid |y - y_0| < r\}$ denote the ball in \mathbb{R}^J of radius $r > 0$ centered at the nominal parameter value y_0 .

Then, for $f \in C^2(B_r(y_0); C^1(\mathbb{R}; \mathbb{R}^d))$ with some $r > 0$ there holds, by Taylor's theorem, for every $u \in \mathbb{R}$, and every $y \in B_r(y_0)$

$$(3.17) \quad f(y; u) = f(y_0; u) + (y - y_0)^\top (\partial_y f)(y_0; u) + O(r^2)$$

so that we may introduce the approximate flux function

$$(3.18) \quad g(y; u) := \bar{f}(u) + y^\top (\partial_y f)(y_0; u)$$

with the *nominal flux* $\bar{f}(u) := f(y_0; u) - y_0^\top (\partial_y f)(y_0; u)$.

We remark that in Example 3.7 we did not require a structural hypothesis (apart from differentiability at the nominal parameter vector y_0) any particular functional form for the dependence of the parametric flux f on the parameter vector y . The approximate flux $g(y; u)$ in (3.18), on the other hand, depends on y in an *affine fashion*.

Example 3.8. (*Karhunen-Loève expansion of bounded random flux*) Consider a bounded random flux $f(\omega; u)$ in the sense of Definition 3.3. By Lemma 3.4, its covariance function $\text{Cov}[f]$ is well-defined; for $0 < R < \infty$ we denote by \mathcal{C}_f^R the integral operator with bi-Lipschitz kernel $\text{Cov}[f](u, v)$, defined on $L^2(-R, R)$ by

$$(3.19) \quad \mathcal{C}_f^R[\Phi](u) := \int_{|v| \leq R} \text{Cov}[f](u, v) \Phi(v) dv.$$

We remark that \mathcal{C}_f^R describes the covariance structure of the random flow on the bounded set $[-R, R]$ of states: as it is well-known from the theory of deterministic scalar conservation laws, given initial data $u_0 \in L^\infty(\mathbb{R}^d)$, by the a-priori bound (3.11) the unique entropy solution $S(t)u_0$ of (3.1) - (3.3) will take values in $[-\|u_0\|_{L^\infty(\mathbb{R}^d)}, \|u_0\|_{L^\infty(\mathbb{R}^d)}]$. For random flux and random initial data, therefore, choosing

$$(3.20) \quad R > \text{ess sup}_{\omega \in \Omega} \|u_0(\omega; \cdot)\|_{L^\infty(\mathbb{R}^d)}$$

will ensure that \mathcal{C}_f^R will “capture” all possible states, \mathbb{P} -almost surely, for the class of initial data under consideration.

For every positive finite constant R , the integral operator \mathcal{C}_f is a compact, self-adjoint operator on $L^2(-R, R)$. By the spectral theorem, it admits for every fixed

value $0 < R < \infty$ a sequence $(\lambda_j^R, \Phi_j^R)_{j \geq 1}$ of real eigenvalues λ_j^R , which assume enumerated in decreasing magnitude and repeated according to multiplicity, which accumulate only at zero, and a corresponding set Φ_j^R of eigenfunctions; to exclude trivial degeneracies, we shall assume throughout that *the sequence $(\Phi_j^R)_{j \geq 1}$ is a complete, orthonormal base of $L^2(-R, R)$.*

It follows from the continuous differentiability (3.15) of covariance function of the random flux, $\text{Cov}[f]$, and from the eigenvalue equation

$$(3.21) \quad (\mathcal{C}_f^R \Phi_j^R)(u) = \lambda_j^R \Phi_j^R(u), \quad |u| \leq R,$$

that $\Phi_j^R \in C^1([-R, R]; \mathbb{R}^d)$: for any $u, u' \in [-R, R]$, there holds by Lemma 3.4 and by the eigenvalue equation (3.21)

$$\begin{aligned} |\Phi_j^R(u) - \Phi_j^R(u')| &= \frac{1}{\lambda_j^R} \left| \int_{-R}^R (\text{Cov}[f](u, v) - \text{Cov}[f](u', v)) \Phi_j^R(v) dv \right| \\ &\leq \frac{1}{\lambda_j^R} \sup_{|v| \leq R} \|\text{Cov}[f](u, v) - \text{Cov}[f](u', v)\|_F \sqrt{2R} \\ &\leq \frac{2B(f)\sqrt{2R}}{\lambda_j^R} \sup_{|v| \leq R} \left(\int_{\Omega} \|f(\omega, v) - \bar{f}(v)\|_2^2 d\mathbb{P}(\omega) \right)^{1/2} |u - u'|. \end{aligned}$$

Any bounded random flux $f(\omega; u)$ therefore admits, for every fixed $0 < R < \infty$, a Karhunen–Loève expansion

$$(3.22) \quad f(\omega; u) = \bar{f}(u) + \sum_{j \geq 1} Y_j^R(\omega) \Psi_j^R(u), \quad |u| \leq R,$$

which converges in $L^2(\Omega; L^2(-R, R)^d)$. We emphasize that the expansion (3.22) is, for $R > 0$ as in (3.20), on the bounded *subset* $[-R, R]$ of the state space \mathbb{R} , rather than on a physical domain of definition of the solution (compare, however, Remark 3.9 ahead). In (3.22), the nominal flux $\bar{f}(u) = \mathbb{E}[f(\cdot; u)]$ and the sequence $(Y_j^R)_{j \geq 1}$ is a sequence of independent random variables given by

$$\forall j \in \mathbb{N}: \quad Y_j^R(\omega) := \sqrt{\lambda_j^R} \int_{|v| < R} f(\omega; v) \Phi_j^R(v) dv.$$

and

$$\forall j \in \mathbb{N}: \quad \Psi_j^R(u) := \frac{1}{\sqrt{\lambda_j^R}} \Phi_j^R(u).$$

We remark that under suitable smoothness conditions on the two-point correlation function $\text{Cov}[f]$ of the random flux the convergence of the expansion (3.22) is *a*) pointwise with respect to u , and *b*) the convergence rates increase with increasing smoothness of $\text{Cov}[f]$ (see, e.g. [26]). For our ensuing numerical analysis, it will be useful to relate the Karhunen–Loève expansion to a parametric, deterministic representation of the random flux, in terms of the principal components of its covariance. To this end, let us denote by $y_j \in [-1, 1]$ the values of rescaled realizations of $Y_j^R(\omega)$ which we denote by $\bar{Y}_j^R(\omega)$. Note that $|y_j| \leq 1$ can always be achieved by rescaling the functions Ψ_j^R in the Karhunen–Loève expansion (3.22) to functions $\bar{\Psi}_j^R$, so that (3.22) takes the form

$$(3.23) \quad f(y; u) = \bar{f}(u) + \sum_{j \geq 1} \bar{Y}_j^R(\omega) \bar{\Psi}_j^R(u), \quad |u| \leq R, \quad y \in U.$$

Here, we denote (by slight abuse of notation) by $f(y; u)$ the random flux $f(\omega; u)$ expressed in terms of the parameters $y_j = Y_j^R$, i.e.,

$$(3.24) \quad f(\omega; u) = f(y; u)|_{y_j = \overline{Y_j^R}(\omega)}, \quad |u| < R.$$

By (3.23), we associate the *parametric, deterministic representation*

$$(3.25) \quad f(y; u) = \bar{f}(u) + \sum_{j \geq 1} y_j \overline{\Psi_j^R}(u), \quad |u| \leq R, \quad y \in U = [-1, 1]^{\mathbb{N}}.$$

We will use the parametric, deterministic form (3.25) of the flux to build *deterministic* numerical solution methods for the random scalar conservation law, instead of sampling methods such as Monte-Carlo Methods as considered in [23, 22]. Before doing so, we present a concrete construction of a probability distribution on the space of all flux functions.

3.5. Probability Measure. On the parameter domain $U = [-1, 1]^{\mathbb{N}}$, we define a probability measure as follows. Let Θ be the σ -algebra defined on U which is generated from the sets of the form $\prod_{j=1}^{\infty} S_j$ where S_j are subintervals of $[-1, 1]$ and only a finite number of them are proper subsets of $[-1, 1]$. On the product sigma algebra Θ , we define the product probability measure

$$d\rho(y) := \otimes_{j \geq 1} dy_j / 2.$$

This construction renders (U, Θ, ρ) is a probability space. As the random coordinates y_j are by assumption independent, identically uniformly distributed, for $S = \prod_{j=1}^{\infty} S_j$,

$$\rho(S) = \prod_{j=1}^{\infty} \mathbb{P}\{\omega : y_j(\omega) \in S_j\}.$$

Remark 3.9. *The Karhunen–Loève expansion (3.23) has been developed for the spatially homogeneous random flux. In the case of spatially inhomogeneous random flux indicated in Remark 3.5, an expansion analogous to (3.23) is available. Here, the principal components $\overline{\Psi_j^R}$ depend on both, the spatial coordinate x and the state u . The parametric, deterministic expansion then takes the form*

$$(3.26) \quad f(y; x, u) = \bar{f}(x, u) + \sum_{j \geq 1} y_j \overline{\Psi_j^R}(x, u), \quad |u| \leq R, \quad y \in U = [-1, 1]^{\mathbb{N}}.$$

3.6. Random Entropy Solution. Based on Theorem 3.1, we will now formulate the SCL (3.1) - (3.3) for random initial data $u_0(\omega; \cdot)$ and random flux $f(\omega; \cdot)$. To this end, we denote $(\Omega, \mathcal{F}, \mathbb{P})$ a probability space. We assume given a Lipschitz continuous random flux $f(\omega; u)$ as in Definition 3.3 and random initial data u_0 , i.e., a $L^1(\mathbb{R}^d)$ -valued random variable which is a $L^1(\mathbb{R}^d)$ measurable map

$$(3.27) \quad u_0 : (\Omega, \mathcal{F}) \mapsto (L^1(\mathbb{R}^d), \mathcal{B}(L^1(\mathbb{R}^d))).$$

We assume further that

$$(3.28) \quad u_0(\omega; \cdot) \in L^\infty(\mathbb{R}^d) \cap BV(\mathbb{R}^d) \quad \mathbb{P}\text{-a.s.},$$

which is to say that

$$(3.29) \quad \mathbb{P}(\{\omega \in \Omega : u_0(\omega; \cdot) \in (L^\infty \cap BV)(\mathbb{R}^d)\}) = 1.$$

Since $L^1(\mathbb{R}^d)$ and $C^1(\mathbb{R}^d; \mathbb{R}^d)$ are separable, (3.27) is well defined and we may impose for $k \in \mathbb{N}$ the *k-th moment condition*

$$(3.30) \quad \|u_0\|_{L^k(\Omega; L^1(\mathbb{R}^d))} < \infty,$$

where the Bochner spaces with respect to the probability measure are defined in Section 2. Then we are interested in random solutions of the *random scalar conservation law* (RSCL)

$$(3.31) \quad \begin{cases} \partial_t u(\omega; x, t) + \operatorname{div}_x(f(\omega; u(\omega; x, t))) = 0, & t > 0, \\ u(\omega; x, 0) = u_0(\omega; x), \end{cases} \quad x \in \mathbb{R}^d.$$

Definition 3.10. A random field $u : \Omega \ni \omega \rightarrow u(\omega; x, t)$, i.e., a measurable mapping from (Ω, \mathcal{F}) to $C([0, T]; L^1(\mathbb{R}^d))$, is a random entropy solution of the SCL (3.31) with random initial data u_0 satisfying (3.27) - (3.30) for some $k \geq 2$ and with a spatially homogeneous random flux $f(\omega; u)$ as in Definition 3.3 that is statistically independent of u_0 , if it satisfies the following,

(i.) *Weak solution:*

For \mathbb{P} -a.e $\omega \in \Omega$, $u(\omega; \cdot, \cdot)$ satisfies the following integral identity,

$$(3.32) \quad \int_0^T \int_{\mathbb{R}^d} \left(u(\omega; x, t) \varphi_t(x, t) + \sum_{j=1}^d f_j(\omega; u(\omega; x, t)) \frac{\partial}{\partial x_j} \varphi(x, t) \right) dx dt \\ + \int_{\mathbb{R}^d} u_0(x, \omega) \varphi(x, 0) dx = 0,$$

for all test functions $\varphi \in C_0^1(\mathbb{R}^d \times [0, T])$.

(ii.) *Entropy condition:*

For any pair of (deterministic) entropy η and (stochastic) entropy flux $Q(\omega; \cdot)$ i.e., η, Q_j with $j = 1, 2, \dots, d$ are functions such that η is convex and such that $Q'_j(\omega; \cdot) = \eta' f'_j(\omega; \cdot)$ for all j , and for \mathbb{P} -a.e $\omega \in \Omega$, u satisfies the following inequality

$$(3.33) \quad \int_0^T \int_{\mathbb{R}^d} \left(\eta(u(\omega; x, t)) \varphi_t(x, t) + \sum_{j=1}^d Q_j(\omega; u(\omega; x, t)) \frac{\partial}{\partial x_j} \varphi(x, t) \right) dx dt \\ + \int_{\mathbb{R}^d} \eta(u_0(\omega; x)) \varphi(x, 0) dx \geq 0,$$

for all deterministic test functions $0 \leq \varphi \in C_0^1(\mathbb{R}^d \times [0, T])$, \mathbb{P} -a.s.

We remark that it is equivalent to assume that (3.33) holds for all Kruřkov entropy functions $\eta(u) = |u - k|$, where k is any constant. Therefore, throughout what follows, we assume that $\eta(u) = |u - k|$. One main result of the present paper is

Theorem 3.11. Consider the SCL (3.1) - (3.3) with spatially homogeneous, bounded random flux $f : \Omega \rightarrow C^1(\mathbb{R}; \mathbb{R}^d)$ as in Definition 3.3 and with (independent of f) random initial data $u_0 : \Omega \rightarrow L^1(\mathbb{R}^d)$ satisfying (3.28), (3.29) and the *k-th moment*

condition (3.30) for some integer $k \geq 2$. In particular, then, there exists a constant $\bar{R} < \infty$ such that

$$(3.34) \quad \|u_0(\omega; \cdot)\|_{L^\infty(\mathbb{R}^d)} \leq \bar{R} \quad \mathbb{P} - \text{a.e. } \omega \in \Omega.$$

Assume moreover that the random flux admits the representation (3.24) with (3.25) where the Lipschitz-continuous scaled flux components $\overline{\Psi}_j^R$ have Lipschitz constants B_j^R such that $\mathbf{B}^R := (B_j^R)_{j \geq 1} \in \ell^1(\mathbb{N})$ with some $R \geq \bar{R}$ as in (3.34).

Then there exists a random entropy solution $u : \Omega \ni \omega \rightarrow C([0, T]; L^1(\mathbb{R}^d))$ which is “pathwise” unique, i.e., for $\mathbb{P} - \text{a.e. } \omega \in \Omega$, described in terms of a nonlinear random mapping $S(\omega; t)$ which depends on ω only through the random flux, such that

$$(3.35) \quad u(\omega; \cdot, t) = S(\omega; t)u_0(\omega; \cdot), \quad t > 0, \mathbb{P} - \text{a.e. } \omega \in \Omega$$

such that for every $k \geq m \geq 1$, for every $0 \leq t \leq T < \infty$, and for \mathbb{P} -a.e. $\omega \in \Omega$

$$(3.36) \quad \|u\|_{L^k(\Omega; C(0, T; L^1(\mathbb{R}^d)))} \leq \|u_0\|_{L^k(\Omega; L^1(\mathbb{R}^d))},$$

$$(3.37) \quad \|S(\omega; t)u_0(\omega; \cdot)\|_{(L^1 \cap L^\infty)(\mathbb{R}^d)} \leq \|u_0(\omega; \cdot)\|_{(L^1 \cap L^\infty)(\mathbb{R}^d)}$$

$$(3.38) \quad TV(S(\omega; t)u_0(\omega; \cdot)) \leq TV(u_0(\omega; \cdot)).$$

and, with \bar{R} as in (3.34),

$$(3.39) \quad \sup_{0 \leq t \leq T} \|u(\omega; \cdot, t)\|_{L^\infty(\mathbb{R}^d)} \leq \bar{R} \quad \mathbb{P} - \text{a.e. } \omega \in \Omega.$$

Proof. We proceed in several steps.

Step 1: We construct candidates for random entropy solution in a “pathwise” fashion, i.e., for \mathbb{P} -a.e. realization of the random flux $f(\omega; \cdot)$, and for given initial condition $u_0(\omega; \cdot)$, there exists a unique entropy solution $u(\omega; x, t) \in C([0, T]; L^1(\mathbb{R}^d))$ of the Cauchy problem (3.2), (3.3) with this realization of the random flux by the existence and uniqueness result Theorem 3.1. By (3.34) and by (3.9), there holds (3.39).

The parametric family of entropy solutions

$$\{u(\omega; \cdot, \cdot) : \mathbb{P} - \text{a.e. } \omega \in \Omega\}$$

is well-defined \mathbb{P} -a.s. by Theorem 3.1 and satisfies (3.39) (which is basis for the Monte-Carlo Finite-Volume approximation to be discussed in the next section). To justify this, it remains to verify that this parametric family of entropy solutions is measurable, i.e., is a random variable taking values in $C([0, T]; L^1(\mathbb{R}^d))$. To do so, we first consider a parametric, deterministic family of SCLs obtained by J -term truncations of the Karhunen–Loève parametrizations (3.22), (3.25) of the random flux. Again by the deterministic existence result, the Cauchy problems (3.2), (3.3) with these parametric, deterministic flux functions will admit unique random entropy solutions.

Moreover, by Theorem 3.2, for truncation to any finite number J of terms, these parametric, deterministic families of entropy solutions will be seen to depend Lipschitz continuously on the parameter vectors $y_j \in [-1, 1]^J$, as mappings from $[-1, 1]^J \mapsto C([0, T]; L^1(\mathbb{R}^d))$. Moreover, the Lipschitz constant will be shown to be uniform with respect to the number J of parameters, which follows from our assumption that $\mathbf{B}^R \in \ell^1(\mathbb{N})$ for some $R \geq \bar{R}$ with \bar{R} as in (3.34).

Step 2: Parametric, deterministic SCL. By assumption the bounded random flux in (3.2) admits the representation (3.24) with the parametric, deterministic flux $f(y; u)$ as in (3.25). For any $y \in U = [-1, 1]^{\mathbb{N}}$, the series (3.25) converges in $C^1(\mathbb{R}; \mathbb{R}^d)$ and its limit is, by the completeness of $C^1(\mathbb{R}; \mathbb{R}^d)$, a continuously differentiable flux function since the sequence $\{f^J\}_{J \geq 1}$ of J -term truncated partial sums, defined by

$$(3.40) \quad f^J(y; u) := \bar{f}(u) + \sum_{j=1}^J y_j \overline{\Psi}_j^R(u), \quad |u| \leq R, \quad y \in U$$

is a (uniformly w.r. to the parameter sequence $y \in U$) Cauchy sequence in $C^1(\mathbb{R}; \mathbb{R}^d)$.

By Theorem 3.1, for each finite truncation order J of the parametric flux function (3.26) there exists a unique entropy solution $u^J(y; x, t)$ of the *parametric, deterministic SCL* (3.2), i.e., of (3.2) with the parametric, deterministic flux $f^J(y; u)$. The same also holds for the limiting problem, where the parametric, deterministic flux $f(y; u)$ is given by (3.23). We denote this parametric entropy solution by $u(y; x, t)$. With the corresponding parametric solution operators $S^J(y; t)$ and $S(y; t)$ as in (3.4), we may write for $J \in \mathbb{N}$

$$(3.41) \quad u(y; \cdot, t) = S(y; t)u_0(\cdot), \quad u^J(y; \cdot, t) = S^J(y; t)u_0(\cdot), \quad t > 0, y \in U.$$

By Theorem 3.2 for every $y \in U$ and every $t > 0$

$$(3.42) \quad \|u(y; t) - u^J(y; t)\|_{L^1(\mathbb{R}^d)} \leq Ct \sum_{j>J} \|\overline{\Psi}_j^R\|_{C^1([-R, R]; \mathbb{R}^d)} \leq Ct \sum_{j>J} B_j^R$$

which tends to zero for $J \rightarrow \infty$ uniformly with respect to $y \in U$ due to our assumption that $B^R \in \ell^1(\mathbb{N})$. By Theorem 3.2, in particular, by the estimate (3.12), $u^J \rightarrow u$ in $C([0, T]; L^1(\mathbb{R}^d))$ as $J \rightarrow \infty$.

Step 3: Candidate random entropy solution.

Motivated by (3.24), we *define* a candidate for the random entropy solution of the SCL (3.2) with bounded random flux by setting, for every $J \in \mathbb{N}$,

$$(3.43) \quad u^J(\omega; x, t) := u^J(y; x, t)|_{y_j = \overline{Y}_j^R(\omega), j=1,2,\dots,J}$$

and then passing to the limit $J \rightarrow \infty$.

Step 4: Measurability.

We verify that the mapping $\Omega \ni \omega \rightarrow u(\omega; x, t)$ defined in (3.43) is measurable as a mapping from the probability space (U, Θ, ρ) introduced in Example 3.8 into the (separable) space $E = C([0, T]; L^1(\mathbb{R}^d))$ equipped with its (natural) sigma algebra of Borel sets $\mathcal{B}(E)$.

By Theorem 3.1, for every $J \in \mathbb{N}$ the parametric, deterministic SCL (3.2) with the (Lipschitz) flux $f^J(y; u)$ defined in (3.40) admits a unique parametric, deterministic entropy solution $u^J(y; x, t)$. Upon inserting here $y_j = \overline{Y}_j^R(\omega)$ for $j = 1, 2, \dots, J$, the resulting random function $u^J(\omega; x, t) := u^J(y; x, t)|_{y_j = \overline{Y}_j^R(\omega), j=1,2,\dots,J}$ is measurable and, by uniqueness, coincides \mathbb{P} -a.s. with the unique entropy solution of the SCL (3.2), with the random flux $f^J(\omega; u) := f^J(y; u)|_{y_j = \overline{Y}_j^R(\omega), j=1,2,\dots,J}$.

Since the sequence $\{f^J\}_{J \geq 1}$ of J -term truncations of the Karhunen–Loève expansion (3.25) is Cauchy in $C^1(\mathbb{R}; \mathbb{R}^d)$ uniformly with respect to the parameter vector $y \in U = [-1, 1]^{\mathbb{N}}$, the continuous dependence result Theorem 3.2 implies that the corresponding sequence $\{u^J(y; x, t)\}_{J \geq 1}$ of (unique) entropy solutions is likewise

Cauchy in $C([0, T]; L^1(\mathbb{R}^d))$. Since $C([0, T]; L^1(\mathbb{R}^d))$ is a (separable) Banach space, for each $y \in U$ there exists a unique limit $\bar{u}(y; \cdot, \cdot) \in C([0, T]; L^1(\mathbb{R}^d))$, and the dependence of this limit on the parameter vector $y \in U$ (equipped with the $\ell^\infty(\mathbb{N})$ norm) is Lipschitz. We may therefore define

$$\bar{u}(\omega; x, t) := \bar{u}(y; x, t)|_{y_j = Y_j^R(\omega), j \geq 1}.$$

Since $\bar{u}(y; x, t)$ is the uniform limit (with respect to $y \in U$) in $E = C([0, T]; L^1(\mathbb{R}^d))$ of the sequence $\{u^J\}_{J \geq 1}$, the function $\bar{u}(\omega; x, t)$ is the uniform in E strong limit of a family of measurable random variables taking values in E , therefore $\bar{u}(\omega; x, t)$ is strongly measurable as mapping from (Ω, \mathcal{F}) into $(E, \mathcal{B}(E))$, hence a random function.

Step 5: Verification of the entropy condition.

Having verified measurability of $\bar{u}(\omega; x, t)$, it remains to show that it satisfies the entropy conditions (3.32), (3.33), \mathbb{P} -a.s. To this end, we first observe that for every $J < \infty$, by construction of the approximate parametric solutions $u^J(y; x, t)$, these solutions satisfy the entropy conditions (3.32), (3.33) pointwise for every $y \in [-1, 1]^J$. Therefore, the random functions $u^J(\omega; x, t) := u^J(y; x, t)|_{y_j = \overline{Y_j^R(\omega)}, j=1, 2, \dots, J}$ satisfy (3.32), (3.33), \mathbb{P} -a.s., for every J . Since the entropy conditions (3.32), (3.33) are stable under strong limits in the space $E = C([0, T]; L^1(\mathbb{R}^d))$, it follows that the limiting functions $\bar{u}(y; x, t)$ and $\bar{u}(\omega; x, t)$ satisfy (3.32), (3.33) for all $y \in U$ resp. \mathbb{P} -a.s.

Step 6: Identification $\bar{u}(\omega; \cdot, \cdot) = u(\omega; x, t)$.

By the uniqueness of the entropy solution, for every $J < \infty$ the random function $u^J(\omega; x, t)$ coincides, in the space $E = C([0, T]; L^1(\mathbb{R}^d))$, \mathbb{P} -a.s. with the ‘‘pathwise’’ entropy solutions of the SCL (3.2), (3.3) with truncated flux functions $f^J(y; u)$ in (3.40). The stability under passage to the limit in E and the uniqueness of entropy solutions complete the proof. \square

Theorem 3.11 generalizes the existence result of [21] where the flux function in (3.2) was assumed to be deterministic. It ensures the existence of a unique random entropy solution $u(\omega; x, t)$ with finite k -th moments for bounded random flux and for independent random initial data u_0 provided that $u_0 \in L^k(\Omega, \mathcal{F}, \mathbb{P}; L^1(\mathbb{R}^d))$.

4. MULTILEVEL MONTE CARLO FINITE VOLUME METHOD

4.1. Monte-Carlo Method. The Monte-Carlo Method is a ‘‘discretization’’ of the SCL random data $f(\omega; u)$, $u_0(\omega; x)$ as in (3.27) - (3.29) with respect to ω . We also assume (3.30), i.e., the existence of k -th moments of u_0 for some $k \in \mathbb{N}$, to be specified later. We shall be interested in the statistical estimation of the first and higher moments of u , i.e., of $\mathcal{M}^k(u) \in (L^1(\mathbb{R}^d))^{(k)}$. For $k = 1$ we obtain the mean field $\mathcal{M}^1(u) = \mathbb{E}[u]$. The *MC approximation of $\mathbb{E}[u]$* is defined as follows: given M independent, identically distributed samples \hat{u}_0^i , $i = 1, \dots, M$, of initial data, the MC estimate of $\mathbb{E}[u(\cdot; \cdot, t)]$ at time t is given by

$$(4.1) \quad E_M[u(\cdot, t)] := \frac{1}{M} \sum_{i=1}^M \hat{u}^i(\cdot, t)$$

where $\widehat{u}^i(\cdot, t)$ denotes the M unique entropy solutions of the M Cauchy Problems (3.1) - (3.3) with initial data \widehat{u}_0^i and flux samples $\widehat{f}^i(\cdot)$. We observe that by

$$(4.2) \quad \widehat{u}^i(\cdot, t) = \widehat{S}^i(t) \widehat{u}_0^i$$

we have from (3.8) - (3.10) for every M and for every $0 < t < \infty$, by (3.10),

$$(4.3) \quad \begin{aligned} \|E_M[u(\omega; \cdot, t)]\|_{L^1(\mathbb{R}^d)} &= \left\| \frac{1}{M} \sum_{i=1}^M \widehat{S}^i(t) \widehat{u}_0^i(\cdot; \omega) \right\|_{L^1(\mathbb{R}^d)} \\ &\leq \frac{1}{M} \sum_{i=1}^M \left\| \widehat{S}^i(t) \widehat{u}_0^i(\omega; \cdot) \right\|_{L^1(\mathbb{R}^d)} \\ &\leq \frac{1}{M} \sum_{i=1}^M \left\| \widehat{u}_0^i(\omega; \cdot) \right\|_{L^1(\mathbb{R}^d)}. \end{aligned}$$

Using the i.i.d. property of the samples $\{\widehat{u}_0^i\}_{i=1}^M$ of the random initial data u_0 , Lemma 2.1 and the linearity of the expectation $\mathbb{E}[\cdot]$, we obtain the bound

$$(4.4) \quad \mathbb{E} \left[\|E_M[u(\cdot; \cdot, t)]\|_{L^1(\mathbb{R}^d)} \right] \leq \mathbb{E} \left[\|u_0\|_{L^1(\mathbb{R}^d)} \right] = \|u_0\|_{L^1(\Omega; L^1(\mathbb{R}^d))} < \infty.$$

As $M \rightarrow \infty$, the MC estimates (4.1) converge in $L^2(\Omega; C([0, T]; L^1(\mathbb{R}^d)))$ and the convergence result from [21] holds as well.

Theorem 4.1. *Assume that in the SCL (3.1) - (3.3) the random initial data u_0 satisfies*

$$(4.5) \quad u_0 \in L^2(\Omega; L^1(\mathbb{R}^d))$$

and that the flux $f(\omega; u)$ is a random flux in the sense of Definition 3.3. Assume further that (3.28), (3.29) hold.

Then the MC estimates $E_M[u(\cdot, t)]$ in (4.1) converge as $M \rightarrow \infty$, to $\mathcal{M}^1(u(\cdot, t)) = \mathbb{E}[u(\cdot, t)]$ and, for any $M \in \mathbb{N}$, $0 < t < \infty$, we obtain the error bound

$$(4.6) \quad \sup_{0 < t < T} \|\mathbb{E}[u(\cdot, t)] - E_M[u(\cdot, t)]\|_{L^2(\Omega; L^1(\mathbb{R}^d))} \leq 2M^{-1/2} \|u_0\|_{L^2(\Omega; L^1(\mathbb{R}^d))}.$$

4.2. Finite Volume Method. So far, we considered the MCM under the assumption that the entropy solutions $\widehat{u}^i(\omega; x, t) = S(\omega; t) \widehat{u}_0^i(\omega; x)$ for the Cauchy problem (3.1) - (3.3) with the random flux samples $f(\omega_i; u)$ and initial data samples $\widehat{u}_0^i = u_0(\omega_i; x)$ are available exactly. In practice, however, numerical approximations of $S(t) \widehat{u}_0^i$ must be computed by FVM. In [21], we analyzed the error of the combined MC-FVM approximations. We recapitulate the classical Kuznetsov type error bounds for first order FVM for the *deterministic* SCL (3.2); these will be required for the convergence statement of the MLMC FVM and also for parametric collocation FVM in the subsequent chapters.

The FVM is based on a time step $\Delta t > 0$ and a triangulation \mathcal{T} of the spatial domain $D \subset \mathbb{R}^d$ of interest. Here, a triangulation \mathcal{T} will be understood as a set of open, convex polyhedra $K \subset \mathbb{R}^d$ with plane faces such that the following conditions hold: the triangulation \mathcal{T} is *shape regular*: if $K \in \mathcal{T}$ denotes a generic volume, we define the volume parameter

$$(4.7) \quad \rho_K = \rho(K) = \max\{\text{diam}(B_r) : B_r \subset \overline{K}\}$$

i.e., the maximum diameter of balls B_r of radius $r > 0$ that can be inscribed into volume \bar{K} for $K \in \mathcal{T}$ and define, in addition, for a generic mesh \mathcal{T} , the *shape regularity constants* (where $\Delta x_K := \text{diam } K$)

$$(4.8) \quad \kappa(\mathcal{T}) := \sup\{\Delta x_K/\rho(K) : K \in \mathcal{T}\}, \quad \mathcal{T} \in \mathfrak{M}.$$

We also denote by $\Delta x(\mathcal{T}) := \max\{\Delta x_K : K \in \mathcal{T}\}$ the *mesh width* of \mathcal{T} . For any volume $K \in \mathcal{T}$, we define the *set $\mathcal{N}(K)$ of neighboring volumes*

$$(4.9) \quad \mathcal{N}(K) := \{K' \in \mathcal{T} : K' \neq K \wedge \text{meas}_{d-1}(\bar{K} \cap \bar{K}') > 0\}.$$

We assume that the triangulation \mathcal{T} are regular in the sense that there exists a constant $B > 0$ independent of $\Delta x(\mathcal{T})$ such that the support size of the FV “stencil” at any element $K \in \mathcal{T}$ is uniformly bounded i.e.,

$$(4.10) \quad \sigma(\mathcal{T}) := \sup_{K \in \mathcal{T}} \#\mathcal{N}(K) \leq B.$$

We introduce the CFL-number

$$(4.11) \quad \lambda = \Delta t/\Delta x(\mathcal{T}).$$

where we implied a uniform discretization in time with constant time step Δt and set $t_n = n\Delta t$. The CFL constant λ is determined by a standard CFL condition (see e.g. [12]) based on the maximum wave speed.

To approximate (3.1)-(3.3), we use a time-explicit, first order FV scheme on \mathcal{T} . It has the general form

$$(4.12) \quad v_K^{n+1} = H(\{v_{K'}^n : K' \in \mathcal{N}(K) \cup K\}), \quad K \in \mathcal{T}$$

where $H : \mathbb{R}^{(2k+1)^d} \rightarrow \mathbb{R}$, with k denoting the size of the stencil of the finite volume scheme, is continuous and where v_K^n denotes an approximation to the cell average of u at time $t_n = n\Delta t$.

In our subsequent developments, we write the FVM in operator form. To this end, we introduce the operator $H_{\mathcal{T}}(v)$ which maps a sequence $\underline{v} = (v_K)_{K \in \mathcal{T}}$ into $H_{\mathcal{T}}((v_K)_{K \in \mathcal{T}})$. Then the FVM (4.12) takes the abstract form

$$(4.13) \quad \underline{v}^{n+1} = H_{\mathcal{T}}(\underline{v}^n), \quad n = 0, 1, 2, \dots$$

For the ensuing convergence analysis, we shall assume and use several properties of the FV scheme (4.13); these properties are satisfied by many commonly used FVM of the form (4.13), on regular or irregular meshes \mathcal{T} in \mathbb{R}^d .

To state the assumptions, we introduce further notation: for any initial data $u_0(x) \in L^1(\mathbb{R}^d)$, we define the FVM approximation $(v_K^0)_{K \in \mathcal{T}}$ by the *cell averages*

$$(4.14) \quad v_K^0 = \frac{1}{|K|} \int_K u_0(x) dx, \quad \text{where } K \in \mathcal{T}.$$

With a vector $\underline{v} = (v_K)_{K \in \mathcal{T}} \in \mathbb{R}^{\#\mathcal{T}}$, we associate the piecewise constant function $v_{\mathcal{T}}(x, t)$ defined a.e. in $\mathbb{R}^d \times (0, \infty)$ by

$$(4.15) \quad v_{\mathcal{T}}(x, t)|_K := v_K^n, \quad K \in \mathcal{T}, \quad t \in [t_n, t_{n+1}).$$

We denote space of all piecewise constant functions on \mathcal{T} (i.e., the “simple” or “step” functions on \mathcal{T}) by $S(\mathcal{T})$. Given any $v_{\mathcal{T}} \in S(\mathcal{T})$, we define the (mesh-dependent) norms:

$$(4.16) \quad \|\underline{v}\|_{L^1(\mathcal{T})} = \sum_{K \in \mathcal{T}} |K| |v_K| = \|v_{\mathcal{T}}\|_{L^1(\mathbb{R}^d)},$$

$$(4.17) \quad \|\underline{v}\|_{L^\infty(\mathcal{T})} = \sup_{K \in \mathcal{T}} |v_K| = \|v_{\mathcal{T}}\|_{L^\infty(\mathbb{R}^d)}.$$

We denote the meshwidth of triangulation \mathcal{T} by

$$(4.18) \quad \Delta x(\mathcal{T}) = \sup\{\text{diam}(K) : K \in \mathcal{T}\}.$$

We shall assume the following properties of the FVM schemes used in the MC-FVM algorithms.

Assumption 4.2. *We shall assume that the abstract FV scheme (4.13) satisfies*

1. Stability: $\forall t \geq 0$

$$(4.19) \quad \|v_{\mathcal{T}}(\cdot, t)\|_{L^\infty(\mathbb{R}^d)} \leq \|v_{\mathcal{T}}(\cdot, 0)\|_{L^\infty(\mathbb{R}^d)},$$

$$(4.20) \quad \|v_{\mathcal{T}}(\cdot, t)\|_{L^1(\mathbb{R}^d)} \leq \|v_{\mathcal{T}}(\cdot, 0)\|_{L^1(\mathbb{R}^d)},$$

$$(4.21) \quad TV(v_{\mathcal{T}}(\cdot, t)) \leq TV(v_{\mathcal{T}}(\cdot, 0)),$$

2. Lipschitz continuity: *For any two sequences $\underline{v} = (v_K)_{K \in \mathcal{T}}$, $\underline{w} = (w_K)_{K \in \mathcal{T}}$ we have*

$$(4.22) \quad \|H_{\mathcal{T}}(\underline{v}) - H_{\mathcal{T}}(\underline{w})\|_{L^1(\mathcal{T})} \leq \|\underline{v} - \underline{w}\|_{L^1(\mathcal{T})}$$

or, equivalently,

$$(4.23) \quad \|H_{\mathcal{T}}(v_{\mathcal{T}}) - H_{\mathcal{T}}(w_{\mathcal{T}})\|_{L^1(\mathbb{R}^d)} \leq \|v_{\mathcal{T}} - w_{\mathcal{T}}\|_{L^1(\mathbb{R}^d)}.$$

3. Convergence: *If the CFL bound $\lambda = \Delta t / \Delta x(\mathcal{T})$ is kept constant as $\Delta x(\mathcal{T}) \rightarrow 0$, the approximate solution $v_{\mathcal{T}}(x, t)$ generated by (4.12) - (4.15) converges to the unique entropy solution u of the scalar conservation laws (3.1) - (3.3) at rate $0 < s \leq 1$, i.e., there exists $C > 0$ independent of Δx such that, as $\Delta x \rightarrow 0$, for every \bar{t} such that, for $(\Delta t)^s \leq \bar{t} \leq T$, it holds*

$$(4.24) \quad \|u(\cdot, \bar{t}) - v_{\mathcal{T}}(\cdot, \bar{t})\|_{L^1(\mathbb{R}^d)} \leq \|u_0 - v_{\mathcal{T}}^0\|_{L^1(\mathbb{R}^d)} + C \bar{t} TV(u_0) \Delta t^s.$$

Let us mention that (4.19), (4.20) and (4.21) do hold for monotone schemes on Cartesian meshes, see [12, 18]. Furthermore, the analysis of Kuznetsov, see e.g. [9], implies that the optimal convergence rate is $s = 1/2$ in (4.24). In case of monotone schemes on general finite volume meshes, one might lose control of the total variation of the approximations, and the convergence rate, i.e., the s in (4.24) drops accordingly, see [5].

Let us also mention that the work for the realization of scheme (4.12) - (4.15) on a bounded domain $D \subset \mathbb{R}^d$ as (using the CFL stability condition (4.11), i.e., $\Delta t / \Delta x(\mathcal{T}) \leq \lambda = \text{const.}$)

$$(4.25) \quad \text{Work}_{\mathcal{T}} = \mathcal{O}(\Delta t^{-1} \Delta x^{-d}) = \mathcal{O}(\Delta x^{-(d+1)}).$$

4.3. MC-FVM. In the Monte Carlo Finite Volume Methods (MC-FVMs), we combine MC sampling of the random initial data with the FVM (4.13). In the convergence analysis of these schemes, we shall require the application of the FVM (4.13) to random initial data $u_0 \in L^\infty(\Omega; L^1(\mathbb{R}^d))$. Given a draw $u_0(x; \omega)$ of u_0 , the FVM (4.13) - (4.15) defines a family $v_{\mathcal{T}}(x, t; \omega)$ of random grid functions.

Proposition 4.3. *Consider the FVM (4.13) - (4.15) for the approximation of the entropy solution corresponding to a draw $u_0(\omega; x)$ of the random initial data and a draw $f(\omega; u)$ of the random flux.*

Then, if the FVM satisfies Assumption 4.2, the random grid functions $\Omega \ni \omega \mapsto v_{\mathcal{T}}(\omega; x, t)$ defined by (4.11) - (4.15) satisfy, for every $0 < \bar{t} < \infty$, $0 < \Delta x < 1$, and every $k \in \mathbb{N} \cup \{\infty\}$, the stability bounds

$$(4.26) \quad \|v_{\mathcal{T}}(\cdot; \cdot, \bar{t})\|_{L^k(\Omega; L^\infty(\mathbb{R}^d))} \leq \|u_0\|_{L^k(\Omega; L^\infty(\mathbb{R}^d))},$$

$$(4.27) \quad \|v_{\mathcal{T}}(\cdot; \cdot, \bar{t})\|_{L^k(\Omega; L^1(\mathbb{R}^d))} \leq \|u_0\|_{L^k(\Omega; L^1(\mathbb{R}^d))}.$$

These bounds hold for all ω . We also have the error bounds

$$(4.28) \quad \begin{aligned} & \|u(\cdot; \cdot, \bar{t}) - v_{\mathcal{T}}(\cdot; \cdot, \bar{t})\|_{L^k(\Omega; L^1(\mathbb{R}^d))} \\ & \leq \|u_0(\cdot; \cdot) - v_{\mathcal{T}}^0(\cdot; \cdot)\|_{L^k(\Omega; L^1(\mathbb{R}^d))} + C\bar{t}\Delta t^s \|TV(u_0(\cdot; \cdot))\|_{L^k(\Omega)}. \end{aligned}$$

We next define and analyze the MC-FVM scheme. It is based on the straightforward idea of generating, possibly in parallel, independent samples of the random initial data and then, for each sample of the random initial data, to perform one FV simulation. The error of this procedure is bound by two contributions: a (statistical) sampling error and a (deterministic) discretization error. We express the asymptotic efficiency of this approach (in terms of overall error versus work). It will be seen that the efficiency of the MC-FVM is, in general, inferior to that of the deterministic scheme (4.13). The present analysis will constitute a key technical tool in our subsequent development and analysis of the multilevel MC-FVM (“MLMC-FVM” for short) which does not suffer from this drawback.

4.3.1. Definition of the MC-FVM Scheme. We consider once more the initial value problem (3.1) - (3.3) with random initial data u_0 satisfying ((3.27) - (3.30) for sufficiently large $k \in \mathbb{N}$ (to be specified in the convergence analysis). The MC-FVM scheme for the MC estimation of the mean of the random entropy solutions then consists in the following:

Definition 4.4. *(MC-FVM Scheme) Given $M \in \mathbb{N}$, generate M i.i.d. samples $\{\hat{u}_0^i\}_{i=1}^M$ of initial data. Let $\{\hat{u}^i(\cdot, t)\}_{i=1}^M$ denote the unique entropy solutions of the scalar conservation laws (3.1) - (3.3) for these data samples, i.e.,*

$$(4.29) \quad \hat{u}^i(\cdot, t) = S(t)\hat{u}_0^i(\cdot), \quad i = 1, \dots, M.$$

Let $H_{\mathcal{T}}(\cdot)$ be a FVM scheme (4.12) - (4.15) satisfying Assumption 4.2. Then the MC-FVM approximations of $\mathcal{M}^k(u(\cdot, t))$ are defined as statistical estimates from the ensemble

$$(4.30) \quad \{\hat{v}_{\mathcal{T}}^i(\cdot, t)\}_{i=1}^M$$

obtained by (4.13) from the FV approximations $\hat{v}_{\mathcal{T}}^i(\cdot, 0)$ of the initial data $\{\hat{u}_0^i(x)\}_{i=1}^M$ samples by (4.14): specifically, the first moment of the random solution $u(\omega; \cdot, t)$ at time $t > 0$, is estimated as

$$(4.31) \quad \mathcal{M}^1(u(\cdot, t)) \approx E_M[v_{\mathcal{T}}(\cdot, t)] := \frac{1}{M} \sum_{i=1}^M \hat{v}_{\mathcal{T}}^i(\cdot, t).$$

4.3.2. *Convergence Analysis of MC-FVM.* We next address the convergence of $E_M[v_{\mathcal{T}}]$ to the mean $\mathbb{E}(u)$.

Theorem 4.5. *Assume that*

$$(4.32) \quad u_0 \in L^\infty(\Omega, L^1(\mathbb{R}^d))$$

and that (3.27) - (3.29) hold. Assume further that we are given a FVM (4.12) - (4.15) such that (4.11) holds and such that Assumption 4.2 is satisfied; in particular, assume that the deterministic FVM scheme converges at rate $s > 0$ in $L^\infty([0, T]; L^1(\mathbb{R}^d))$ for every $0 < T < \infty$. Then the MC estimate $E_M[v_{\mathcal{T}}(\cdot, t)]$ defined in (4.31) satisfies, for every M , the error bound

$$(4.33) \quad \begin{aligned} & \|\mathbb{E}[u(\cdot, t)] - E_M[v_{\mathcal{T}}(\omega; \cdot, t)]\|_{L^2(\Omega; L^1(\mathbb{R}^d))} \\ & \leq C \left[M^{-\frac{1}{2}} \|u_0\|_{L^2(\Omega; L^1(\mathbb{R}^d))} \right. \\ & \quad \left. + \|u_0 - v_{\mathcal{T}}^0\|_{L^\infty(\Omega; L^1(\mathbb{R}^d))} + t \Delta t^s \|TV(u_0(\omega; \cdot))\|_{L^\infty(\Omega)} \right] \end{aligned}$$

where $C > 0$ is independent of M and of Δt as $M \rightarrow \infty$ and as $\lambda \Delta x = \Delta t \downarrow 0$. The convergence rate $\Delta x^s > 0$ is as in (4.24).

Theorem 4.5 was proved (for deterministic flux functions) in [?]. The proof for random flux functions is a straightforward modification of the corresponding arguments presented in [?].

4.3.3. *Work estimates.* For computational purposes, we have to assume that the computational domain $D \subset \mathbb{R}^d$ is bounded and suitable boundary conditions are specified on ∂D . Noting that in a bounded domain D , the work for one time step (4.12), (4.13) is of order $\mathcal{O}(\Delta x^{-d})$ (with $\mathcal{O}(\cdot)$ depending on the size of the domain), we find from the CFL condition (4.11) that the total computational work to obtain $\{v_{\mathcal{T}}(\cdot, t)\}_{0 < t \leq T}$ in D is by (4.25)

$$(4.34) \quad \text{Work}(\mathcal{T}) = \mathcal{O}(\Delta x^{-d-1}), \quad \text{as } \lambda \Delta x = \Delta t \downarrow 0,$$

which implies that the work for the computation of the MC estimate $E_M[v_{\mathcal{T}}(\cdot, t)]$ is

$$(4.35) \quad \text{Work}(M, \mathcal{T}) = \mathcal{O}(M \Delta x^{-d-1}), \quad \text{as } \Delta t = \lambda \Delta x \downarrow 0,$$

so that we obtain from (4.33) the convergence order in terms of work: to this end we equilibrate in (4.33) the two bounds by choosing $M^{-1/2} \sim \Delta t^s$, i.e., $M = \Delta t^{-2s}$. Inserting in (4.35) yields

$$(4.36) \quad \text{Work}(\mathcal{T}) = \mathcal{O}(\Delta t^{-2s} \Delta x^{-(d+1)}) \stackrel{(4.11)}{=} \mathcal{O}(\Delta x^{-(d+1)-2s})$$

so that we obtain from (4.33)

$$(4.37) \quad \|\mathbb{E}[u(\cdot, t)] - E_M[v_{\mathcal{T}}(\cdot, t)]\|_{L^2(\Omega; L^1(\mathbb{R}^d))} \leq C \Delta t^s \leq C (\text{Work}(\mathcal{T}))^{-s/(d+1+2s)}.$$

We sum up the foregoing considerations.

Remark 4.6. (Work vs. accuracy of MC-FVM) Let us add some comments on the exponent in (4.37). In the *deterministic FV scheme*, we obtain

$$\text{Work}(\mathcal{T}) = \mathcal{O}(\Delta t^{-1} \Delta x^{-d}) \stackrel{(4.11)}{=} \mathcal{O}(\Delta x^{-(d+1)}),$$

and the error in terms of work bound (4.24) becomes

$$(4.38) \quad \begin{aligned} & \|u(\cdot, \bar{t}) - v_{\mathcal{T}}(\cdot, \bar{t})\|_{L^1(\mathbb{R}^d)} \\ & \leq \|u_0 - v_{\mathcal{T}}^0\|_{L^1(\mathbb{R}^d)} + C\bar{t}TV(u_0) (\text{Work}(\mathcal{T}))^{-s/(d+1)}. \end{aligned}$$

Assuming exact representation of the initial data, we obtain the exponent $-s/(d+1)$ for the deterministic FVM as compared to $-s/(d+1+2s)$ for the MC-FVM. We see in particular in the (typical) situation of low order s of convergence and space dimension $d=2, 3$ a considerably reduced rate of convergence of the MC-FVM, in terms of accuracy vs. work, is obtained. On the other hand, for high order schemes (i.e., when $s \gg d+1$) the MC error dominates and we recover in (4.38) the rate $1/2$ in terms of work which is typical of MC methods.

4.4. Multilevel MC-FVM. Next, we present and analyze a scheme that allows us to achieve almost the accuracy versus work bound (4.38) of the deterministic FVM also for the stochastic initial data u_0 and stochastic flux function f , rather than the single level MC-FVM error bound (4.37). The key ingredient in the Multilevel Monte Carlo Finite Volume (MLMC-FVM) scheme is simultaneous MC sampling on different levels of resolution of the FVM, *with level dependent numbers M_ℓ of MC samples*. To define these, we introduce some notation.

4.4.1. Notation. The MLMC-FVM is defined as a *multilevel discretization* in x and t with level dependent numbers M_ℓ of samples. To this end, we assume we are given a family $\{\mathcal{T}_\ell\}_{\ell=0}^\infty$ of *nested triangulations* of \mathbb{R}^d such that the mesh width

$$(4.39) \quad \Delta x_\ell = \Delta x(\mathcal{T}_\ell) = \sup\{\text{diam}(K) : K \in \mathcal{T}_\ell\} = \mathcal{O}(2^{-\ell}\Delta x_0), \quad \ell \in \mathbb{N}_0,$$

where K denotes a generic finite volume cell $K \in \mathcal{T}$. We also assume the family $\mathfrak{M} = \{\mathcal{T}_\ell\}_{\ell=0}^\infty$ of meshes to be shape regular; if $K \in \mathcal{T}_\ell$ denotes a generic cell, we recall, for a generic mesh $\mathcal{T} \in \mathfrak{M}$, the *shape regularity constants* $\kappa(\mathcal{T})$ defined in (4.8). We say that *the family \mathfrak{M} of meshes is κ -shape regular*, if there exists a constant $\kappa(\mathfrak{M}) < \infty$ such that with ρ_K denoting the diameter of the largest ball inscribed into K

$$(4.40) \quad \kappa(\mathfrak{M}) = \sup_{\mathcal{T} \in \mathfrak{M}} \kappa(\mathcal{T}) = \sup_{\mathcal{T} \in \mathfrak{M}} \sup_{K \in \mathcal{T}} \frac{\text{diam}(K)}{\rho_K}.$$

For a mesh hierarchy $\mathfrak{M} = \{\mathcal{T}_\ell\}_{\ell=0}^\infty$, we denote

$$(4.41) \quad \Delta x_\ell := \Delta x(\mathcal{T}_\ell), \quad \mathcal{T}_\ell \in \mathfrak{M}, \quad \ell = 0, 1, \dots$$

4.4.2. Derivation of MLMC-FVM. As in plain MC-FVM, our aim is to estimate, for $0 < t < \infty$, the expectation (or “ensemble average”) $\mathbb{E}[u(\cdot, t)]$ of the random entropy solution of the SCL (3.1) - (3.3) with random initial data $u_0(\omega; \cdot)$, $\omega \in \Omega$, satisfying (3.27) - 3.30 for sufficiently large values of k (to be specified in the sequel). As in the previous section, $\mathbb{E}[u(\cdot, t)]$ will be estimated by replacing $u(\cdot, t)$ by a FVM approximation. For $\ell \in \mathbb{N}_0$, we denote in the present section the FV approximation $v_{\mathcal{T}}$ by $v_\ell(\cdot, t)$ on mesh $\mathcal{T}_\ell \in \mathfrak{M}$, where we assume that the CFL condition (4.11) takes the form

$$(4.42) \quad \Delta t_\ell \leq \lambda \Delta x_\ell, \quad \ell = 0, 1, 2, \dots,$$

with a constant $\lambda > 0$ which is independent of ℓ .

By the stability of the FVM scheme, we generate a sequence $\{v_\ell(\cdot, t)\}_{\ell=0}^\infty$ of stable FV approximations on triangulation \mathcal{T}_ℓ for time steps of sizes Δt_ℓ which satisfy the CFL condition (4.42) with respect to grid $\mathcal{T}_\ell \in \mathfrak{M}$. We set in what

follows $v_{-1}(\cdot, t) := 0$. Then, given a target level $L \in \mathbb{N}$ of spatial resolution, we may use the linearity of the expectation operator to write

$$(4.43) \quad \mathbb{E}[v_L(\cdot, t)] = \mathbb{E}\left[\sum_{\ell=0}^L (v_\ell(\cdot, t) - v_{\ell-1}(\cdot, t))\right].$$

We next estimate each term in (4.43) statistically by a multi-level Monte-Carlo method with a level-dependent number of samples, M_ℓ ; this gives the MLMC-FVM estimator

$$(4.44) \quad E^L[u(\cdot, t)] = \sum_{\ell=0}^L E_{M_\ell} [v_\ell(\cdot, t) - v_{\ell-1}(\cdot, t)]$$

where $E_M[v_{\mathcal{T}}(\cdot, t)]$ is as in (4.31), and where $v_\ell(\cdot, t)$ denotes the grid-function on mesh \mathcal{T}_ℓ , computed under the assumption (4.42), i.e., that the time steps Δt_ℓ are chosen subject to the CFL constraint (4.11).

4.4.3. *Convergence Analysis.* The MLMC-FVM mean field error

$$(4.45) \quad \|\mathbb{E}[u(\cdot, t)] - E^L[u(\cdot, t)]\|_{L^2(\Omega; L^1(\mathbb{R}^d))}$$

for $0 < t < \infty$ and $L \in \mathbb{N}$ was analyzed in [21] for the SCL (3.2) with random initial data and deterministic flux. Analogous results hold for the more general SCL with random flux (3.31): The choice of the sample sizes $\{M_\ell\}_{\ell=0}^\infty$ such that, for every $L \in \mathbb{N}$, the MLMC error (4.45) is of order $(\Delta t_L)^s$, where s is the order of convergence in the Kuznetsov type error bound (4.24). The principal issue in the design of MLMC-FVM is the optimal choice of $\{M_\ell\}_{\ell=0}^\infty$ such that, for each L , an error (4.45) is achieved with minimal total work given by (based on (4.35))

$$(4.46) \quad \text{Work}_L = \sum_{\ell=0}^L M_\ell \mathcal{O}(\Delta x_\ell^{-d-1}) = \mathcal{O}\left(\sum_{\ell=0}^L M_\ell \Delta x_\ell^{-d-1}\right).$$

As in [?], we arrive at the error bound

$$\|(v_\ell - v_{\ell-1})(\cdot, t)\|_{L^2(\Omega; L^1(\mathbb{R}^d))} \leq C \left\{ t \|TV(u_0)\|_{L^2(\Omega)} + \Delta x_\ell^s \|u_0\|_{L^2(\Omega; W^{s,1}(\mathbb{R}^d))} \right\}.$$

Summing this error bound over all discretization levels $\ell = 0, \dots, L$, we obtain

Theorem 4.7. *Assume (3.1) - (3.3), (3.27) - (3.30) and (4.40) - (4.42). Then, for any sequence $\{M_\ell\}_{\ell=0}^\infty$ of sample sizes at mesh level ℓ , we have for the MLMC-FVM estimate $E^L[u(\cdot, t)]$ in (4.44) the error bound*

$$(4.47) \quad \begin{aligned} & \|\mathbb{E}[u(\cdot, t)] - E^L[u(\cdot, t)]\|_{L^2(\Omega; L^1(\mathbb{R}^d))} \\ & \leq C \left\{ \bar{t} \Delta x_L^s \|TV(u_0)\|_{L^1(\Omega)} + \Delta x_L^s \|u_0\|_{L^\infty(\Omega; W^{s,1}(\mathbb{R}^d))} \right\} \\ & \quad + C \left\{ \sum_{\ell=0}^L M_\ell^{-\frac{1}{2}} \Delta x_\ell^s \right\} \left\{ \|u_0\|_{L^2(\Omega; W^{s,1}(\mathbb{R}^d))} + t \|TV(u_0)\|_{L^2(\Omega)} \right\}, \end{aligned}$$

where C is a constant independent of L and s .

Theorem 4.7 was proved (for deterministic flux functions) in [21]. The proof for random flux functions is a straightforward modification of the corresponding arguments presented in [21]. It is the basis for an optimization of the numbers M_ℓ of MC samples across the mesh levels which yields the same result for random flux and random initial data, as for the case of deterministic flux and random initial

data considered in [21]. The level dependent selection of the Monte Carlo sample sizes M_ℓ proposed in [21] is based on the last term in the error bound (4.47): we select in (4.47) the M_ℓ such that as $\Delta t \downarrow 0$, all terms equal the Kuznetsov bound Δt_L^s in (4.24) at the finest level L resulting in

$$(4.48) \quad M_\ell^{-\frac{1}{2}} \Delta x_\ell^s = \hat{C} \Delta x_L^s, \quad \ell = 0, \dots, L-1.$$

Here, \hat{C} is some positive integer constant that is independent of l and of L .

As in [21] and under the assumption that $s < \frac{d+1}{2}$, we obtain the following error estimate in terms of work

$$(4.49) \quad \|\mathbb{E}[u(\cdot, t)] - E^L[u(\cdot, t)]\|_{L^1(\mathbb{R}^d)} \leq C (\text{Work}(M_L; \mathcal{T}_L))^{-s/(d+1)} \log(\text{Work}(M_L; \mathcal{T}_L))$$

5. STOCHASTIC COLLOCATION FVM

We now describe an alternative, *deterministic* approach to the numerical solution of the SCL with random flux. It is based on deterministic collocation approximation of the parametric, deterministic SCL

$$(5.1) \quad \partial_t u(y; x, t) + \text{div}_x(f(y; u(y; x, t))) = 0 \quad \text{for } (x, t) \in \mathbb{R}^d \times [0, T] \text{ and } y \in U,$$

where the parametric flux function $f(y; u)$ is as in (3.25). We note that the parameter space $U = [-1, 1]^{\mathbb{N}}$ is, in general, *infinite-dimensional*. Moreover, by Theorem 3.11 the parametric SCL (5.1) admits, for every $y \in U$, a unique random entropy solution $u(y; x, t)$. The parametric SCL (5.1) is *equivalent* to the RSCL (3.31) via the identification

$$(5.2) \quad u(\omega; x, t) = u(y; x, t)|_{y_j = Y_j^R(\omega)}.$$

5.1. Regularity of the random entropy solution. Given a finite Karhunen–Loève truncation index $J \in \mathbb{N}$ and $t > 0$, the random entropy solution $u^J(\cdot, t; \omega)$ can be determined, according to (3.43), by the numerical solution of the *deterministic, parametric SCL*

$$(5.3) \quad \frac{\partial u^J}{\partial t} + \text{div}_x f^J(y; u) = 0 \quad \text{in } \mathbb{R}^d \times \mathbb{R}_+ \text{ and } y \in U.$$

To quantify the parameter dependence of u^J we fix $y \in U$ and denote, for $1 \leq j \leq J < \infty$, by $\tilde{y}^{(j)}$ a perturbation of y in the j th component only, i.e., $y_i^{(j)} = y_i$ for all $i \neq j$. Then

$$\forall u \in \mathbb{R}^d : \quad f^J(\tilde{y}^{(j)}; u) - f^J(y; u) = (\tilde{y}_j - y_j) \overline{\Psi}_j^R$$

and by Theorem 3.2 estimate (3.12), we find the a-priori bound

$$\forall t > 0, y \in U : \quad \left\| u^J(\tilde{y}^{(j)}; \cdot, t) - u^J(y; \cdot, t) \right\|_{L^1(\mathbb{R}^d)} \leq Ct |y_j - \tilde{y}_j| B_j^R$$

which implies that the random entropy solution depends Lipschitz-continuously on the parameter y_j and that

$$(5.4) \quad \forall t > 0 : \quad \left\| \partial_{y_j} u^J(\cdot; \cdot, t) \right\|_{L^\infty([-1, 1]^J; L^1(\mathbb{R}^d))} \leq Ct B_j^R, \quad j = 1, 2, \dots, J.$$

Here $C > 0$ depends only on u_0 and the Lipschitz constant of the random flux, but is independent of j, J, t .

We remark that estimate (5.4) could be used to scale the meshwidths in coordinate y_j in the sFVM, in terms of the (bounds on) principal components of the flux.

5.2. Stochastic Collocation. We now propose a collocation type approximation of the parametric SCL (5.3). Since we work under mere Lipschitz continuity of the random flux, the dependence of the entropy solution of (5.3) on the parameter vector y is, in general, not better than Lipschitz; in particular, under the Lipschitz assumptions on the random flux, *we do not have at our disposal in general a so-called “mixed regularity” of the parametric entropy solution* which is necessary for high convergence rates of sparse tensor collocation approximations. We therefore now propose and analyze an *anisotropic*, full-tensor collocation approximation in the parameter domain $[-1, 1]^J$ for Lipschitz functions with a sequence $\mathbf{B} = (B_j)_{j \geq 1}$ of coordinate-wise Lipschitz constants B_j which we assume to be enumerated in decreasing magnitude, i.e.,

$$(5.5) \quad 1 = B_1 \geq B_2 \geq \dots, \quad \mathbf{B} = (B_j)_{j \geq 1} \in \ell^1(\mathbb{N}).$$

We start the construction of our interpolation in one dimension. Consider a stepsize $h > 0$ and a function $g \in C^1([-h, h])$. Then the constant “interpolant” $I_h[g] = g(0)$ of g satisfies for every $x \in [-h, h]$:

$$|g(x) - I_h[g]| = |g(x) - g(0)| \leq 2hC^1(g).$$

Here, $C^1(g)$ denotes the Lipschitz constant of g . Taking the supremum over $x \in [-h, h]$ in this inequality, we find

$$(5.6) \quad \|g - I_h[g]\|_{L^\infty(-h, h)} \leq 2C^1(g)h.$$

Translation of this estimate implies

Lemma 5.1. *Assume that $g \in C^1([-1, 1])$. For $h = 1/N$ with $N \in \mathbb{N}$ denote by $I_h[g]$ the step-function approximation of g obtained by collocating g at the midpoints of the N subintervals of $[-1, 1]$ of length $2h$, i.e., at $-1 + (2j - 1)h$, $j = 1, 2, \dots, N$. The operator $I_h[\cdot]$ is bounded*

$$(5.7) \quad \forall g \in C^1([-1, 1]) \forall h : \|I_h[g]\|_{L^\infty(-1, 1)} \leq \|g\|_{L^\infty(-1, 1)},$$

and we have the error estimate

$$(5.8) \quad \|g - I_h[g]\|_{L^\infty(-1, 1)} \leq h \|g'\|_{L^\infty(-1, 1)}.$$

In the multivariate domain $[-1, 1]^J$ with $J > 1$, we interpolate analogously, but in an *anisotropic fashion*: to this end, we denote by I_j the univariate interpolation operator I_h from Lemma 5.1, applied to a function $g(y) \in C^1([-1, 1]^J)$ with respect to coordinate y_j , for $1 \leq j \leq J$ and with stepsize h_j . We can and will assume in the following that the stepsizes h_j can differ between coordinate directions. We also denote by $\mathbf{h} = (h_1, \dots, h_J)$ the vector of coordinate-wise stepsizes, and by

$$(5.9) \quad \mathcal{I}_{\mathbf{h}} = \bigotimes_{1 \leq j \leq J} I_j$$

the interpolation operator on the axiparallel, tensor product interpolation grid with stepsizes \mathbf{h} in $[-1, 1]^J$. It will be convenient at times to interpolate functions $g(y)$ of countably many variables $y = (y_j)_{j \geq 1}$. In this case, we *assume that only finitely many stepsizes h_j in \mathbf{h} are strictly less than 1, say h_1, h_2, \dots, h_J for some $J \in \mathbb{N}$, and that $h_j = 1$ for all $j > J$* . Then, for all parameters $j > J$, we understand collocation with respect to co-ordinate y_j to require only one collocation point given

by $y_j = 0$. With this understanding, the number of interpolation points is still finite and given by

$$(5.10) \quad N(\mathbf{h}) = \prod_{j \geq 1} h_j^{-1}$$

where the formally infinite product is well-defined as

$$(5.11) \quad \forall j > J : h_j = 1 \Rightarrow \forall j > J : y_j = 0.$$

We now present an error bound for $\mathcal{I}_{\mathbf{h}}$.

Lemma 5.2. *Assume that $g \in C^1(U)$, $U = [-1, 1]^{\mathbb{N}}$, and that the sequence $\mathbf{B} = (B_j)_{j \geq 1}$ of coordinate-wise Lipschitz constants defined by*

$$B_j = \sup_{(y_i)_{i \geq 1} \in U} |(\partial_{y_j}^1 g)(y_1, y_2, \dots)|, \quad j = 1, 2, \dots,$$

of g satisfies $1 = B_1 \geq B_2 \geq \dots$ and $\mathbf{B} \in \ell^1(\mathbb{N})$.

Then for any vector \mathbf{h} of stepsizes $h_j \in (0, 1]$ with $h_j = 1$ for all $j > J$ for some $J \in \mathbb{N}$ there holds the error bound

$$\|g - \mathcal{I}_{\mathbf{h}}[g]\|_{L^\infty(U)} \leq \sum_{j \geq 1} h_j B_j.$$

This is proved by using the univariate error bound (5.8) and induction on the number of dimensions.

The stochastic collocation approximation of the random SCL (3.31) will be based on applying the interpolation operator $\mathcal{I}_{\mathbf{h}}$ to the (or equivalently by (5.2)) parametric SCL (5.3). Note that (5.3) is formally obtained by truncating the parametric random flux $f(y; u)$ in (3.25) to J terms. However, it is easily verified that *the interpolation $\mathcal{I}_{\mathbf{h}}$ achieves the J -term truncation by (5.11)*. Application of the tensor product interpolant $\mathcal{I}_{\mathbf{h}}$ defined in (5.9) to the parametric SCL (5.3) is effected by solving it numerically with the FVM from Section 4.2 such that (4.11) - (4.15) hold, *with the same mesh \mathcal{T} and identical timestep Δt for each collocation point $(y_1, \dots, y_J, 0, 0, \dots)$.*

Under Assumption 4.2, this choice of collocation points and time steps results in a discretization error bound (4.24) which is uniform for all collocation points and in work $O(\Delta x^{-d-1})$ per collocation point. To estimate the total complexity of this procedure, it remains to multiply by the number $N(\mathbf{h})$ in (5.10) of collocation points. We next estimate $N(\mathbf{h})$. To do so, we recall (5.4) and fix a tolerance $0 < h \leq 1$. We equilibrate the coordinate contributions to the error bound by choosing $B_j = CtB_j^R$ and by requiring

$$\forall j \geq 1 : \quad h = h_j B_j = CtB_j^R h_j.$$

Based on Assumption 4.2 we choose $h = \Delta x^s$. This implies

$$(5.12) \quad h_j := h/B_j^R \wedge 1 \Rightarrow h_j^{-1} = 1 \wedge h^{-1} B_j^R, \quad j \geq 1.$$

Since the sequence $(B_j^R)_{j \geq 1}$ is related to the covariance function of the random flux, it is decreasing to zero with rate which depends on the smoothness of this covariance as a function of the states u, u' . We analyze complexity under two scenarios: *i*) exponential decay: $B_j^R = \exp(-\bar{b}j)$ and *ii*) algebraic decay: $B_j^R = j^{-\beta}$ for $j \geq 1$ and some $\beta > 1$. In case *i*) we find from (5.12) that

$$h_j = 1 \text{ for } j > J(h; \mathbf{B}) = \lceil \log h \rceil / \bar{b}.$$

Inserting this into (5.10) we find that

$$N(\mathbf{h}) = \prod_{1 \leq j \leq J} h^{-1} \exp(-\bar{b}j) = h^{-J} \exp\left(-\bar{b} \sum_{j=1}^J j\right) \sim \exp(J |\log h| - \bar{b}J^2/2).$$

Using $J = |\log h|/\bar{b}$ we find in case *i*) (exponential Karhunen–Loève eigenvalue decay)

$$N(\mathbf{h}) \sim \exp(|\log h|^2/2\bar{b}).$$

In case *ii*), a similar analysis using Stirling’s formula yields

$$N(\mathbf{h}) \sim \exp\left(\beta h^{-1/\beta}\right).$$

These bounds indicate that in both cases the curse of dimensionality is present, but also that large parameters \bar{b} and β indicate a weak dependence on the dimension as the discretization parameter $h \downarrow 0$.

6. NUMERICAL EXPERIMENTS

Next, we test both the Multi-level Monte Carlo (MLMC) and the Stochastic collocation finite volume (SFV) methods, developed in the last sections with a series of numerical tests.

6.1. One-dimensional case. To this end, we consider the following one-dimensional scalar conservation law:

$$(6.1) \quad \frac{\partial u}{\partial t} + \frac{\partial f(\omega; u)}{\partial x} = 0, \quad x \in (0, L), \quad t > 0;$$

$$(6.2) \quad u(x, 0) = u_0(x),$$

with random flux function,

$$(6.3) \quad f(\omega; u) = \frac{u^2}{2} + \delta \left(\sum_{j \geq 1} Y_j(\omega) \sqrt{\lambda_j} \Phi_j(u) \right),$$

where $\Phi_j(u)$ and λ_j are the eigenfunctions and eigenvalues of an integral operator defined on $D = [-R, R]$ by a covariance kernel $C_Y(u_1, u_2)$, i.e.,

$$\int_D C_Y(u_1, u_2) \Phi(u_1) du_1 = \lambda \Phi(u_2), \quad u_2 \in D.$$

For definiteness, we choose the following *exponential* covariance kernel,

$$C_Y(u_1, u_2) = \sigma_Y^2 e^{-|u_1 - u_2|/\eta},$$

the corresponding eigenvalues and eigenfunctions are given by,

$$(6.4) \quad \lambda_j = \frac{2\eta\sigma_Y^2}{\eta^2 w_j^2 + 1}, \quad \Phi_j(u) = \frac{1}{\sqrt{(\eta^2 w_j^2 + 1)L/2 + \eta}} [\eta w_j \cos(w_j u) + \sin(w_j u)],$$

where w_j are the roots of

$$(\eta^2 w^2 - 1) \sin(wL) = 2\eta w \cos(wL)$$

Furthermore, we choose the random variables Y_j to be uniformly distributed i.e.,

$$Y_j \in \mathcal{U}(0, 1),$$

and reparametrize the random sequence by $\mathbf{y} = (y_1, y_2, \dots) = \mathbf{Y}(\omega) = (Y_1(\omega), Y_2(\omega), \dots)$ to obtain the following parametric conservation law, Then

$$f(\omega; u) = f(\mathbf{y}; u) \Big|_{\mathbf{y}=\mathbf{Y}(\omega)} = \frac{u^2}{2} + \delta \left(\sum_{j \geq 1} y_j \sqrt{\lambda_j} \Phi_j(u) \right).$$

Furthermore, the coefficients λ_j in the expansion (6.4) decay quickly w.r.t. j as $\lambda_j \sim j^{-k}$ with $k \approx 2.5$ (see Figure 1).

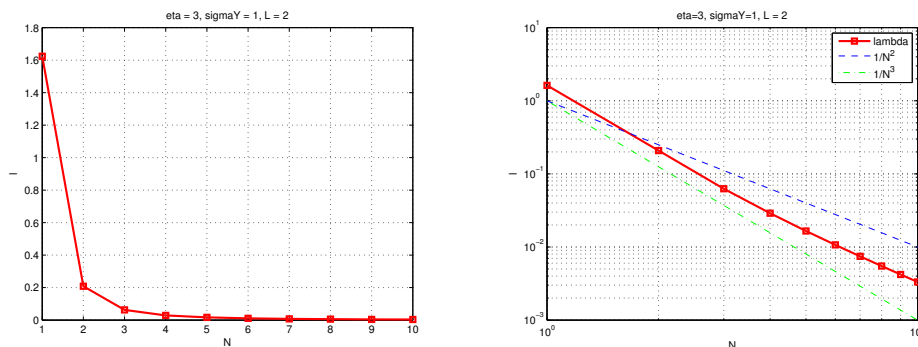


FIGURE 1. Eigenvalues in linear (left) and doubly logarithmic (right) axes

Therefore the expansion (6.3) can be truncated at moderate number of terms ($q = 2, 3$) without losing too much information about the stochastic process. Hence, the resulting flux function is

$$f(\mathbf{y}; u) = \frac{u^2}{2} + \delta \left(\sum_{j=1}^q y_j \sqrt{\lambda_j} \Phi_j(u) \right).$$

In the ensuing numerical experiments, we assume $\delta = 0.2$ which ensures strict convexity of the flux function for all possible realizations. This is used, in particular, to easily compute reference solutions for sufficiently small time (before shock formation) via the method of characteristics. It should be emphasized that strict convexity is not necessary for our theory to apply or our numerical methods to work. A typical path-wise flux function, used in our computation, is plotted in Fig. 2.

We also choose the deterministic initial data,

$$u_0(x) = 1 + \sin(\pi x)$$

and periodic boundary conditions.

We compute the approximate random entropy solutions with the stochastic collocation finite volume method of the previous section. The results at time $t = 0.1$ are shown in figure 3. A typical path wise solution is shown in the left. As seen from the figure, the path wise solution is still smooth at this early time as the wave has not yet steepened to form a shock. The mean of the solution (as well as mean \pm standard deviation) are shown in the right of figure 3. Given the smoothness of pathwise solutions at this early time, the mean remains smooth. Furthermore, the variance is quite low and is concentrated in the middle region of the sign wave.

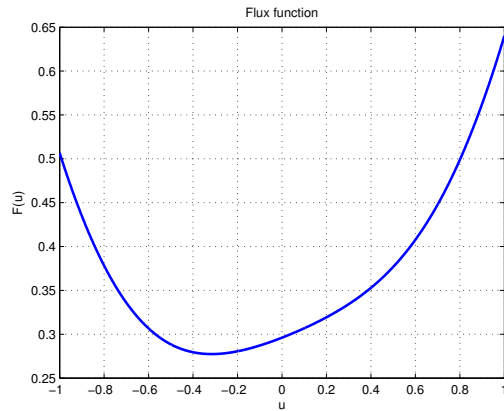
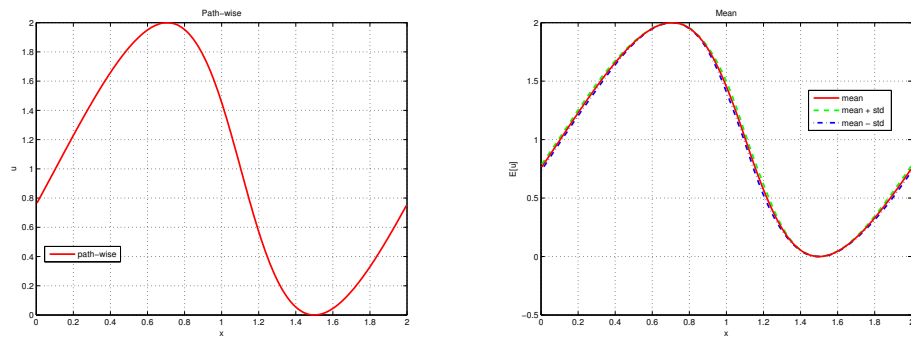


FIGURE 2. Typical realization of the random flux

FIGURE 3. Typical sample path of the random solution (left) and mean and mean \pm standard deviation of the random solution (right) at $t = 0.1$ for the uniformly distributed random flux function.

Numerical results for the approximate random entropy solutions at time $T = 0.5$ are shown in figure 4. A typical path wise solution is shown in the left of this figure. At this late time, the wave has steepened to form a shock wave in the middle, bordered by rarefactions and this structure is reflected in the path wise solution. The mean is shown in the right of figure 4. The mean appears to more regular than a typical path wise solution. Furthermore, the variance has increased considerably. It is non-trivial throughout the domain but has a larger amplitude near the shock. The regularity of mean might be attributed to the subtle smoothing of stochastic shock profiles, see [27].

In Fig. 5 (left), we plot the error for the mean of the random entropy solution in $L^1(\mathcal{R})$ at time $T = 0.1$ with a third-order WENO3 method as the choice of spatial discretization. The results show the correct rate of convergence of the method. Further, to illustrate the anisotropic mesh selection procedure of the last section,

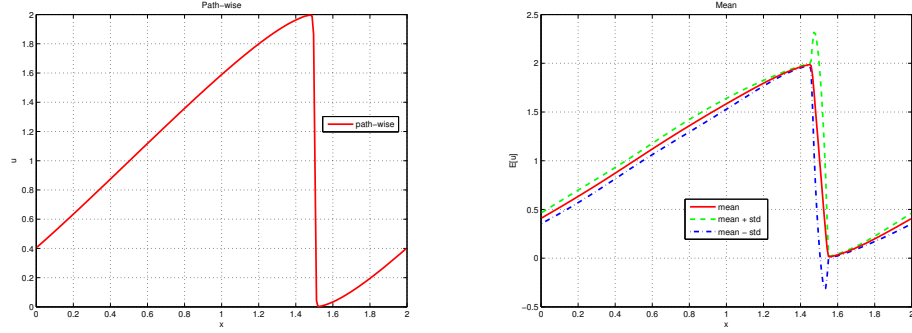


FIGURE 4. Typical sample path of the random solution (left) and mean and mean \pm standard deviation of the random solution (right) at $t = 0.5$ for the uniformly distributed random flux function.

we choose an anisotropic (weighted according to the expansion weights, as proposed in the last section) and present the corresponding $L^1(\mathcal{R})$ error as a function of mesh resolution. As seen in the figure, the adapted method (based on anisotropic mesh selection) performs as well (in terms of spatial resolution) as the method based on uniform mesh in the stochastic variables. However, the substantial efficiency gain is visible when inspecting the CPU time, shown in Fig. 5 (right). This gain in efficiency demonstrates the utility of the anisotropic mesh selection procedure.

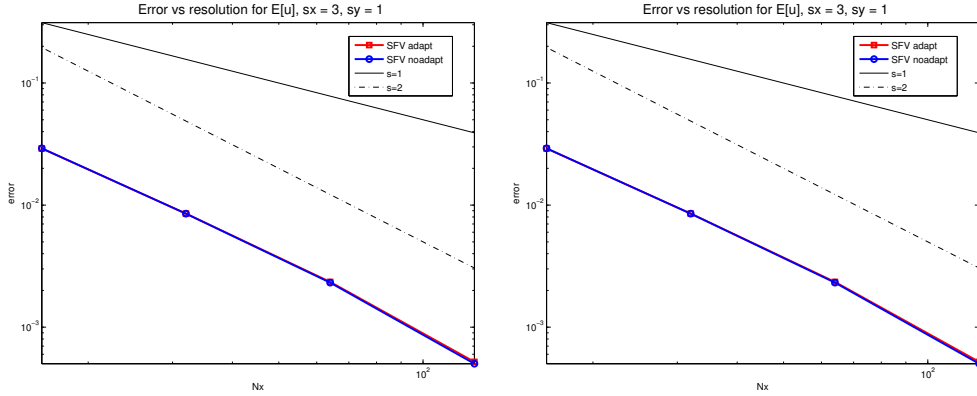


FIGURE 5. $L^1(\mathcal{R})$ Error in mean vs .resolution (left) and vs. computational time (right)

In the next example, we retain the previous set-up but change the random coefficients in the expansion (6.3) to be normally distributed, i.e.,

$$Y_j \sim \mathcal{N}(0, 1), \quad \mathbb{E}[Y_j Y_k] = \delta_{jk}.$$

We remark that in this case, the random flux function is no longer uniformly bounded. Hence, the theory developed in the paper is no directly applicable to

this case. However, we would like to investigate whether the numerical methods developed by us apply to this rather difficult configuration. To this end, we apply the stochastic collocation finite volume method and present results in Fig. 6 where we illustrate one typical configuration of the path-wise solution and the solution mean at time $t = 0.2$. For this computation, we have used a 5-th order WENO solver in the spatial variable and a third-order strong stability preserving (SSP) Runge-Kutta solver for time integration, on a uniform mesh of 64 cells. Note that the time step is determined by the standard CFL condition. The figure shows a pathwise solution that is still smooth. The initial sinus wave is steepening but has not yet steepened into a shock wave. In Fig. 7, we demonstrate the convergence results for the solution mean. We plot the error vs. resolution as well as the error vs. computational time in this figure. The spatial discretizations considered are first order finite volume, second order ENO and third and fifth order WENO schemes. The numerical results clearly show that increasing the order of the underlying spatial discretization increases the efficiency (by reducing CPU time while maintaining numerical accuracy) of the method. In figure 8, we present convergence results for

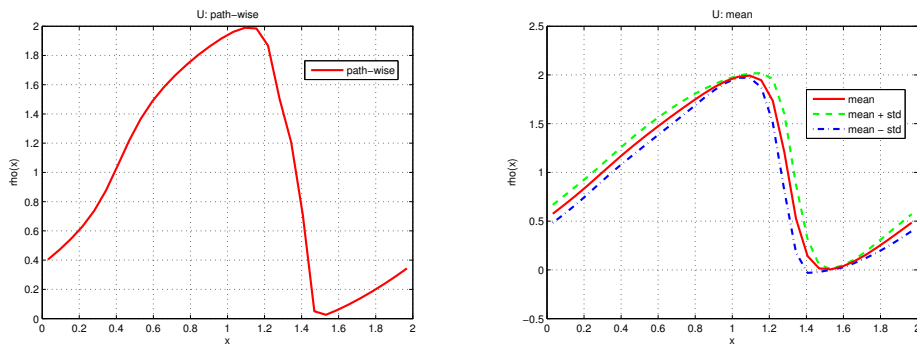


FIGURE 6. Typical sample path of the random solution (left) and mean and mean \pm standard deviation of the random solution (right) at $t = 0.2$

the variance of the solution. Note that the stochastic collocation method is able to approximate the variance quite well too.

Fig. 9 illustrates a discontinuous path-wise solution and the solution mean at $t = 0.5$, i.e. after shock formation. As in previous case, we note that the solution mean in this case is a smooth function.

The results with an anisotropic mesh selection are presented in Figures. 10 and 11. The time of comparison in Figure 10 is $t = 0.1$. At this time, most of the path-wise solutions are smooth and the shock is yet to be formed. The same spatial and temporal solvers are used for both calculations– the only difference being the comparison between the anisotropic mesh (selected by the Karhunen–Loève expansion of the flux) and an isotropic mesh. As predicted by the theory and observed for the previous numerical experiment, the anisotropic mesh selection increases efficiency considerably by reducing the computational time (to compute a similar error level) by at least one order of magnitude, when compared with the isotropic mesh. Furthermore, in Figure 11, we show the convergence results at time $t = 0.5$ (well after

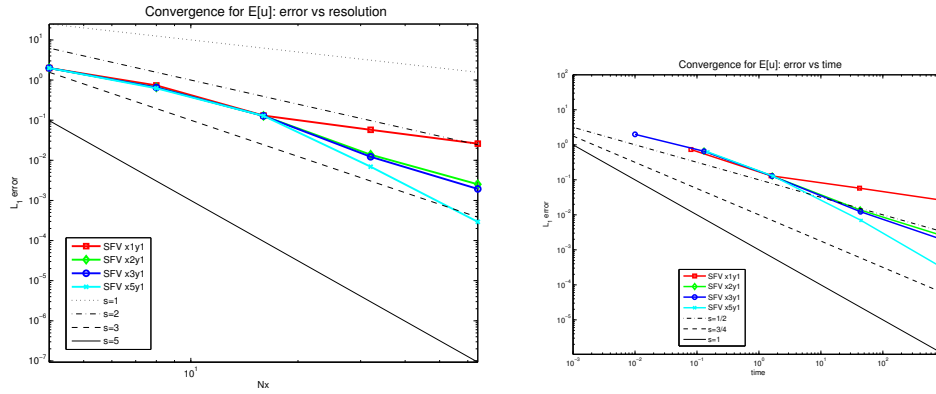


FIGURE 7. Convergence of the stochastic collocation FV method for the solution mean: $L^1(\mathbb{R})$ -error vs. number of cells in space (left) and vs. CPU time (right)

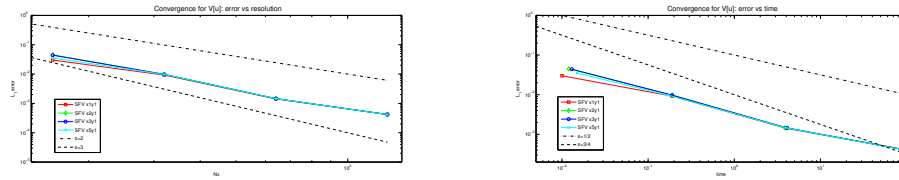


FIGURE 8. Convergence of the stochastic collocation FV method for the solution variance: $L^1(\mathbb{R})$ -error vs. number of cells in space (left) and vs. CPU time (right)

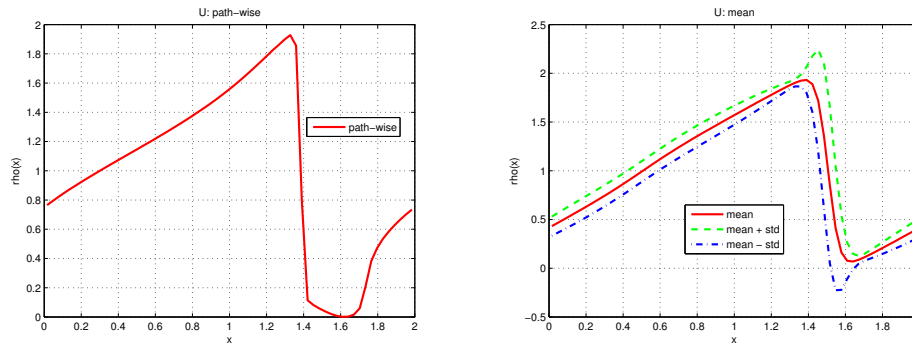


FIGURE 9. Typical sample path of the random solution (left) and mean and mean \pm standard deviation of the random solution (right) at $t = 0.5$

shock formation) and demonstrate that the presence of shocks does not impede the efficiency gained by using the anisotropic mesh selection procedure. Even at this

later time, anisotropic mesh selection offers an order of magnitude speedup over the isotropic mesh.

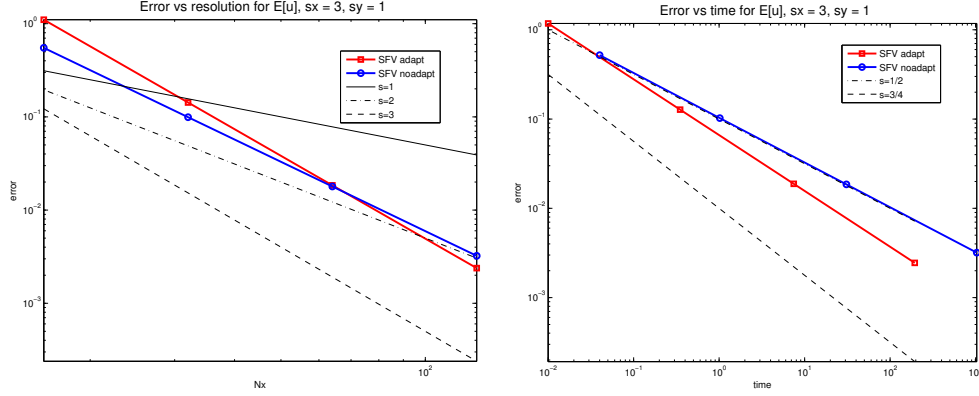


FIGURE 10. Efficiency of the Karhunen–Loève -based mesh adaptation at $t = 0.1$ (smooth solution): $L^1(\mathbb{R})$ -error vs. number of cells in space (left) and vs. CPU time (right)

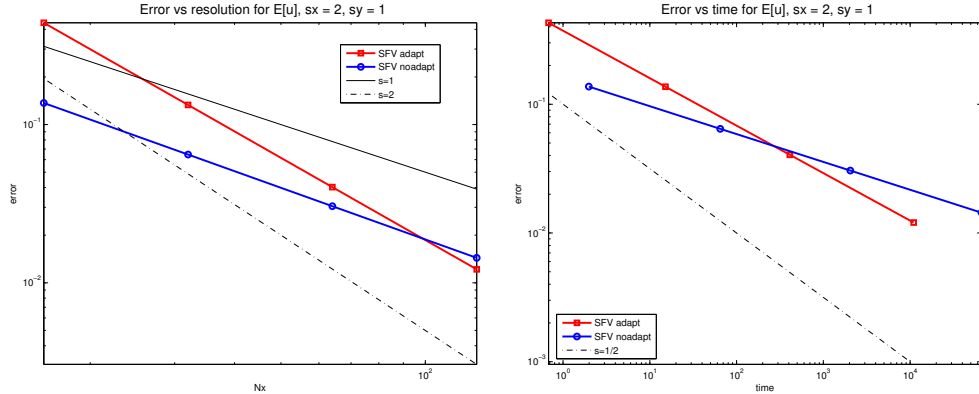


FIGURE 11. Efficiency of the KL-based mesh adaptation at $t = 0.5$ (shock solution): $L^1(\mathbb{R})$ -error vs. number of cells in space (left) and vs. CPU time (right)

So far, we have presented numerical results only with stochastic collocation Finite Volume (FV) method. Next, we compare this method with the Multi-level Monte Carlo (MLMC) FV method that was proposed in section 4. Again the same initial data and flux function are used as in the previous numerical experiment. The following four schemes are compared: i) a MLMC approximation with first order spatio-temporal discretization, ii) a MLMC approximation with a second order spatio-temporal discretization, iii) a stochastic collocation approximation with first order finite volume spatio-temporal discretization, iv) a stochastic collocation approximation with a second order finite volume spatio-temporal discretization. All

the four schemes are compared with respect to error vs. resolution as well as error vs. computational time at $t = 0.1$ (time before shock formation, \mathbb{P} almost surely) in Figure 12. The figure shows that the second order spatio-temporal discretizations have better resolution than the first-order discretizations. Furthermore, the MLMC FV approximation is more accurate at the resolutions that we consider. However, given the empirical convergence rates one can expect at finer mesh resolutions the stochastic collocation approximation will be more accurate. We emphasize that these findings are based on the anisotropic mesh version of the stochastic collocation method. The MLMC FV method is clearly more efficient in terms of computational time when compared with the stochastic collocation FV method. While some of this efficiency gain can be attributed to the fact that different codes are used for different methods with the MLMC code being optimized, the very nature of Multi level Monte Carlo type methods do suggest that they are computationally efficient for problems with low spatial regularity. Similar efficiency gains are also observed with the MLMC FV method when the approximate solutions are compared at a later time $t = 0.5$ (well past shock formation). These results are shown in Figure 13. In the CPU-time versus error comparisons of the MLMC FV in these figures it is to be borne in mind that these results were obtained with two different implementations, and also on different computing hardware.

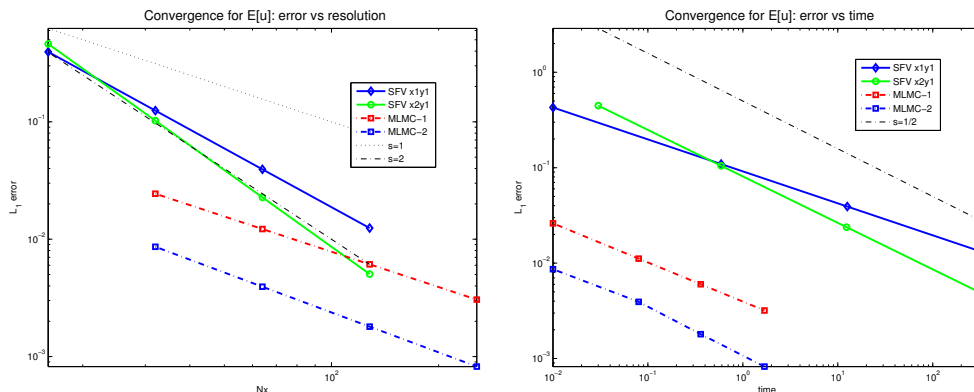


FIGURE 12. Convergence of stochastic collocation FV and MLMC methods at $t = 0.1$: $L^1(\mathbb{R})$ -error vs. number of cells in space (left) and vs. CPU time (right)

Two-dimensional scalar conservation law. We consider the two-dimensional scalar conservation law with random fluxes and deterministic initial data:

$$(6.5) \quad \frac{\partial u}{\partial t} + \frac{\partial f(\omega; u)}{\partial x_1} + \frac{\partial g(\omega; u)}{\partial x_2} = 0, \quad (x_1, x_2) \in (0, L_1) \times (0, L_2), \quad t > 0;$$

$$(6.6) \quad u(x_1, x_2, 0) = u_0(x_1, x_2),$$

where the fluxes are

$$f(\omega; u) = \frac{|u|^{p_1(\omega)}}{p_1(\omega)}$$

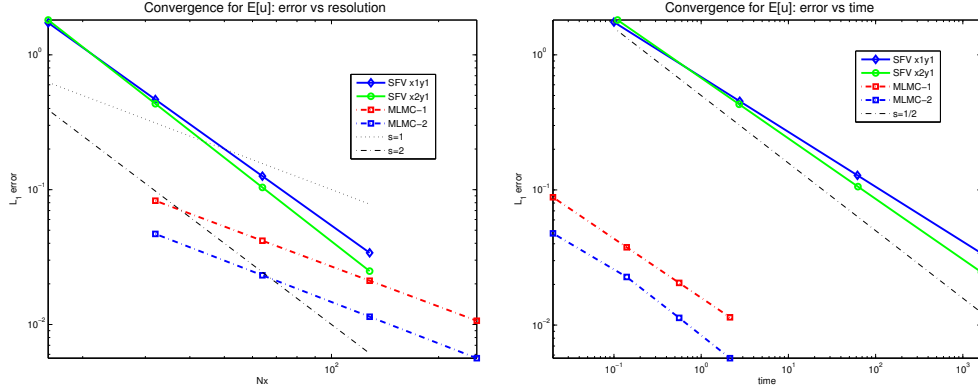


FIGURE 13. Convergence of stochastic collocation FV and MLMC methods at $t = 0.5$: $L^1(\mathbb{R})$ -error vs. number of cells in space (left) and vs. CPU time (right)

with $p_1(\omega) \sim \mathcal{U}[1, 3]$ and

$$g(\omega; u) = \frac{|u|^{p_2(\omega)}}{p_2(\omega)}$$

with $p_2(\omega) \sim \mathcal{U}[1, 3]$.

We choose $u_0(x_1, x_2)$ as follows:

$$u_0(x_1, x_2) = \begin{cases} 1, & \text{if } |x_1 - x_1^s| < 0.4, |x_2 - x_2^s| < R_s; \\ -1, & \text{if } (x_1 - x_2^c)^2 + (x_2 - x_2^c)^2 < R_c^2; \\ 0, & \text{otherwise.} \end{cases}$$

We apply the stochastic collocation FV method based on 5th order WENO solver in the physical space to solve (6.5)–(6.6) with $L_1 = L_2 = 2.0$, $x_1^s = x_2^s = 0.5$, $R_s = 0.4$, $x_1^c = x_2^c = 1.5$ and $R_c^2 = 0.4$ on the 64×64 Cartesian grid. The computational results for $t = 1.0$ are presented in Fig. 14 and show that the SCFVM approximates the pathwise solution as well as statistical moments of the random solution in a robust manner.

7. CONCLUSION

Scalar conservation laws with random initial data as well as random flux functions are considered in this paper. An appropriate notion of random entropy solutions is proposed and these solutions are shown to exist under the assumption that the random flux function is (almost surely in the probability space) bounded as well as continuously differentiable. A novel Karhunen–Loève expansion on the state space is proposed and used to generate approximate (parametric, deterministic) solutions for the random conservation law. Two sets of numerical methods are analysed i) a Multi-level Monte Carlo finite volume method (MLMCFVM) and ii) a stochastic collocation finite volume method (SCFVM). Both methods are shown to converge and numerical experiments demonstrating them are presented. In particular, the sensitivity analysis of the solution for the random conservation law suggests a novel anisotropic mesh selection strategy that improves the complexity

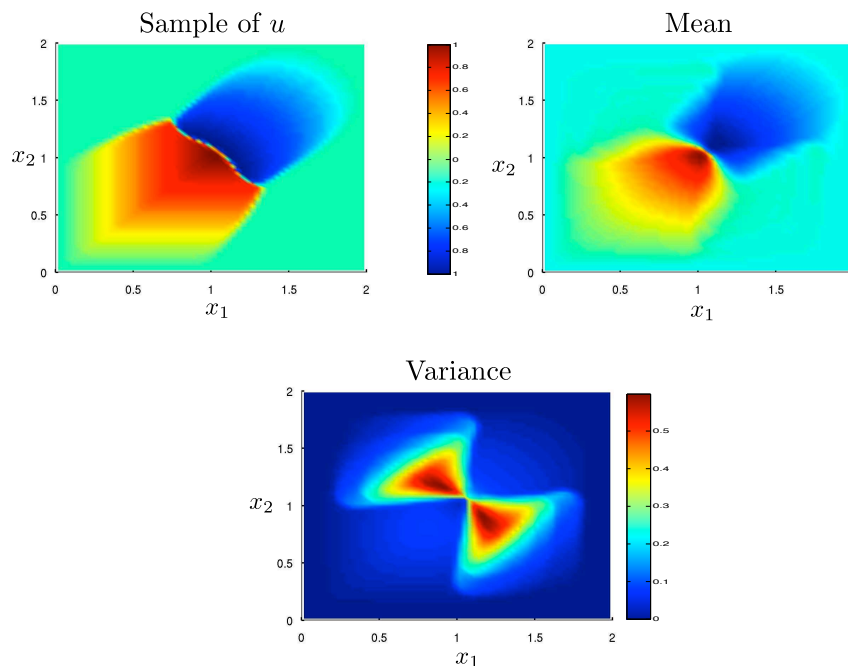


FIGURE 14. Computed sample path (upper left), mean (upper right) and variance (bottom) of the random solution to (6.5)–(6.6) at $t = 0.5$

of the SCFVM. Extensions of these numerical methods to systems of conservation laws with random fluxes with detailed numerical experiments can be found in [29] and in [22].

REFERENCES

- [1] R. Abgrall. A simple, flexible and generic deterministic approach to uncertainty quantification in non-linear problems. INRIA preprint, 2007.
- [2] A. Barth, C. Schwab, and N. Zollinger. Multi-level Monte Carlo finite element method for elliptic PDEs with stochastic coefficients. *Numer. Math.*, 119(1):123–161, 2011.
- [3] T. J. Barth. On the propagation of statistical model parameter uncertainty in CFD calculations. *Theor. Comp. Fluid. Dynamics*, 26:435–457, 2012.
- [4] Q.-Y. Chen, D. Gottlieb, and J. S. Hesthaven. Uncertainty analysis for the steady-state flows in a dual throat nozzle. *J. Comput. Phys.*, 204(1):378–398, 2005.
- [5] B. Cockburn, F. Coquel, and P. G. LeFloch. Convergence of the finite volume method for multidimensional conservation laws. *SIAM J. Numer. Anal.*, 32(3):687–705, 1995.
- [6] G. Da Prato and J. Zabczyk. *Stochastic equations in infinite dimensions*, volume 44 of *Encyclopedia of Mathematics and its Applications*. Cambridge University Press, Cambridge, 1992.
- [7] C. M. Dafermos. *Hyperbolic conservation laws in continuum physics*, volume 325 of *Grundlehren der Mathematischen Wissenschaften [Fundamental Principles of Mathematical Sciences]*. Springer-Verlag, Berlin, third edition, 2010.
- [8] W. E, K. Khanin, A. Mazel, and Y. Sinai. Invariant measures for Burgers equation with stochastic forcing. *Ann. of Math. (2)*, 151(3):877–960, 2000.

- [9] R. Eymard, T. Gallouët, and R. Herbin. Finite volume methods. In *Handbook of numerical analysis, Vol. VII*, Handb. Numer. Anal., VII, pages 713–1020. North-Holland, Amsterdam, 2000.
- [10] M. Giles. Improved multilevel Monte Carlo convergence using the Milstein scheme. In *Monte Carlo and quasi-Monte Carlo methods 2006*, pages 343–358. Springer, Berlin, 2008.
- [11] M. B. Giles. Multilevel Monte Carlo path simulation. *Oper. Res.*, 56(3):607–617, 2008.
- [12] E. Godlewski and P.-A. Raviart. *Hyperbolic systems of conservation laws*, volume 3/4 of *Mathématiques & Applications (Paris) [Mathematics and Applications]*. Ellipses, Paris, 1991.
- [13] E. Godlewski and P.-A. Raviart. *Numerical approximation of hyperbolic systems of conservation laws*, volume 118 of *Applied Mathematical Sciences*. Springer-Verlag, New York, 1996.
- [14] S. Heinrich. Multilevel Monte Carlo methods. In *Large-scale scientific computing*, pages 58–67. Springer, Berlin, 2001.
- [15] H. Holden, T. Lindstrøm, B. Øksendal, J. Ubøe, and T.-S. Zhang. The Burgers equation with a noisy force and the stochastic heat equation. *Comm. Partial Differential Equations*, 19(1-2):119–141, 1994.
- [16] H. Holden and N. H. Risebro. Conservation laws with a random source. *Appl. Math. Optim.*, 36(2):229–241, 1997.
- [17] H. Holden and N. H. Risebro. *Front tracking for hyperbolic conservation laws*, volume 152 of *Applied Mathematical Sciences*. Springer, New York, 2011. First softcover corrected printing of the 2002 original.
- [18] D. Kröner. *Numerical schemes for conservation laws*. Wiley-Teubner Series Advances in Numerical Mathematics. John Wiley & Sons Ltd., Chichester, 1997.
- [19] R. J. LeVeque. *Finite volume methods for hyperbolic problems*. Cambridge Texts in Applied Mathematics. Cambridge University Press, Cambridge, 2002.
- [20] G. Lin, C. H. Su, and G. E. Karniadakis. The stochastic piston problem. *Proc. Natl. Acad. Sci. USA*, 101(45):15840–15845 (electronic), 2004.
- [21] S. Mishra and C. Schwab. Sparse tensor multi-level monte carlo finite volume methods for hyperbolic conservation laws with random initial data. *Math. Comp.*, 81:1979–2018, 2012.
- [22] S. Mishra, C. Schwab, and J. Šukys. Multi-level Monte Carlo finite volume methods for uncertainty quantification in nonlinear systems of balance laws, *Lecture Notes in Computational Science and Engineering*, **92**, 225–294, (2013)
- [23] S. Mishra, C. Schwab, and J. Šukys. Multi-level monte carlo finite volume methods for non-linear systems of conservation laws in multi-dimensions. *J. Comput. Phys.*, 231:3365–3388, 2012.
- [24] G. Poëtte, B. Després, and D. Lucor. Uncertainty quantification for systems of conservation laws. *J. Comput. Phys.*, 228(7):2443–2467, 2009.
- [25] N. H. Risebro, C. Schwab, and F. Weber. Multilevel monte-carlo front tracking for random scalar conservation laws. Research Report 2012-17, Seminar for Applied Mathematics, ETH Zürich (in review).
- [26] C. Schwab and R. A. Todor. Karhunen-Loève approximation of random fields by generalized fast multipole methods. *J. Comput. Phys.*, 217(1):100–122, 2006.
- [27] C. Schwab and S. Tokareva. High order approximation of probabilistic shock profiles in hyperbolic conservation laws with uncertain initial data. M2AN Mathematical Modelling and Numerical Analysis (2012).
- [28] J. Smoller. *Shock waves and reaction-diffusion equations*, volume 258 of *Grundlehren der Mathematischen Wissenschaften [Fundamental Principles of Mathematical Sciences]*. Springer-Verlag, New York, second edition, 1994.
- [29] S. Tokareva. Numerical solution of conservation laws with random flux, PhD Dissertation ETH Zürich, ETH Diss Nr. 21498, 2013.
- [30] J. Troyen, O. Le Maitre, M. Ndjinga, and A. Ern. Intrusive projection methods with upwinding for uncertain non-linear hyperbolic systems. Preprint, 2011.
- [31] X. Wan and G. E. Karniadakis. Long-term behavior of polynomial chaos in stochastic flow simulations. *Comput. Methods Appl. Mech. Engrg.*, 195(41-43):5582–5596, 2006.
- [32] J. Wehr and J. Xin. White noise perturbation of the viscous shock fronts of the Burgers equation. *Comm. Math. Phys.*, 181(1):183–203, 1996.
- [33] J. Wehr and J. Xin. Front speed in the Burgers equation with a random flux. *J. Statist. Phys.*, 88(3-4):843–871, 1997.

(Siddhartha Mishra)
SEMINAR FOR APPLIED MATHEMATICS
ETH
HG G. 57.2,
RÄMISTRASSE 101, ZÜRICH, SWITZERLAND.
E-mail address: `smishra@sam.math.ethz.ch`

(Nils Henrik Risebro)
CENTRE OF MATHEMATICS FOR APPLICATIONS (CMA)
UNIVERSITY OF OSLO, P.O.BOX-1053, BLINDERN, OSLO-0316, NORWAY.
E-mail address: `nilshr@math.uio.no`

(Christoph Schwab)
SEMINAR FOR APPLIED MATHEMATICS
ETH
HG G. 57.1,
RÄMISTRASSE 101, ZÜRICH, SWITZERLAND.
E-mail address: `schwab@sam.math.ethz.ch`

(Svetlana Tokareva)
SEMINAR FOR APPLIED MATHEMATICS
ETH
HG E. 62.2,
RÄMISTRASSE 101, ZÜRICH, SWITZERLAND.
E-mail address: `svetlana.tokareva@sam.math.ethz.ch`

Recent Research Reports

Nr.	Authors/Title
2012-25	F. Y. Kuo and Ch. Schwab and I. H. Sloan Multi-level quasi-Monte Carlo finite element methods for a class of elliptic partial differential equations with random coefficients
2012-26	H. Heumann and R. Hiptmair Stabilized Galerkin methods for magnetic advection
2012-27	P. Grohs Wolfowitz's theorem and consensus algorithms in Hadamard spaces
2012-28	E. Fonn and P. Grohs and R. Hiptmair Hyperbolic cross approximation for the spatially homogeneous Boltzmann equation
2012-29	A. Abdulle and A. Barth and Ch. Schwab Multilevel Monte Carlo methods for stochastic elliptic multiscale PDEs
2012-30	G. M. Coclite and L. Di Ruvo and J. Ernest and S. Mishra Convergence of vanishing capillarity approximations for scalar conservation laws with discontinuous fluxes
2012-31	A. Madrane and U. S. Fjordholm and S. Mishra and E. Tadmor Entropy conservative and entropy stable finite volume schemes for multi-dimensional conservation laws on unstructured meshes
2012-32	A. Lang and S. Larsson and Ch. Schwab Covariance structure of parabolic stochastic partial differential equations
2012-33	R. Hiptmair and C. Jerez-Hanckes and S. Mao Extension by zero in discrete trace spaces: Inverse estimates
2012-34	R. Hiptmair and Ch. Schwab and C. Jerez-Hanckes Sparse tensor edge elements